

Title: Nogo-A does not inhibit retinal axon regeneration in the lizard, *Gallotia galloti*

Running title: Nogo-A during lizard optic nerve regeneration

Authors: Dirk M. Lang^{1*}, Maria del Mar Romero-Alemán², Bryony Dobson¹, Elena Santos², Maximina Monzón-Mayor²

Institutional affiliations: ¹Division of Physiological Sciences, Department of Human Biology.

University of Cape Town, Observatory 7925, South Africa. ²Research Institute of Biomedical and Health Sciences, University of Las Palmas de Gran Canaria, 35016 Las Palmas (Canary Islands, Spain).

Number of text pages: 26

Number of figures: 7

Supplementary figures: 0

Number of tables: 1

*Correspondence to: Dr. Dirk M. Lang, Division of Physiological Sciences, Department of Human Biology, University of Cape Town, Observatory 7925, South Africa. Tel. +27-21-4066419, e-mail: dirk.lang@uct.ac.za

This article has been accepted for publication and undergone full peer review but has not been through the copyediting, typesetting, pagination and proofreading process which may lead to differences between this version and the Version of Record. Please cite this article as an 'Accepted Article', doi: 10.1002/cne.13525

© 2016 Wiley Periodicals, Inc.

Received: Nov 18, 2015; Revised: Jun 19, 2016; Accepted: Jul 08, 2016

ABSTRACT

The myelin-associated protein Nogo-A contributes to the failure of axon regeneration in the mammalian CNS. Inhibition of axon growth by Nogo-A is mediated by the Nogo-66 receptor (NgR). Non-mammalian vertebrates, however, are capable of spontaneous CNS axon regeneration, and we have shown that retinal ganglion cell (RGC) axons regenerate in the lizard, *Gallotia galloti*. Using immunohistochemistry, we observed spatiotemporal regulation of Nogo-A and NgR in cell bodies and axons of RGCs during ontogeny. In the adult lizard, expression of Nogo-A was associated with myelinated axon tracts and up-regulated in oligodendrocytes during RGC axon regeneration. NgR became up-regulated in RGCs following optic nerve injury.

In *in vitro* studies, Nogo-A-Fc failed to inhibit growth of lizard RGC axons. The inhibitor of pKA activity, KT5720 blocked growth of lizard RGC axons on substrates of Nogo-A-Fc, but not laminin. On patterned substrates of Nogo-A-Fc, KT5720 caused restriction of axon growth to areas devoid of Nogo-A-Fc. cAMP levels were elevated over sustained periods in lizard RGCs following optic nerve lesion.

We conclude that Nogo-A and NgR are expressed in a mammalian-like pattern and up-regulated following optic nerve injury, but presence of Nogo-A does not inhibit RGC axon regeneration in the lizard visual pathway. The results of outgrowth assays suggest that outgrowth-promoting substrates and activation of the cAMP/pKA signaling pathway play a key role in spontaneous lizard retinal axon regeneration in the presence of Nogo-A. Restriction of axon growth by patterned Nogo-A-Fc substrates suggests that Nogo-A may contribute to axon guidance in the lizard visual system.

Keywords: neurite growth inhibitor; development; axon regeneration; optic pathway; reptile;
RRID: AB_10000211; RRID: AB_1620281; RRID: AB_257899; RRID: AB_1620281; RRID:
AB_357520; AB_2314901; RRID: AB_2619717; RRID: AB_477010; RRID: AB_11211656;
RRID: SCR_002677; RRID: SCR_002078

INTRODUCTION

Retinal ganglion cells (RGCs) can regenerate their axons in fish, amphibians and certain species of reptiles, but not in mammals. The failure of axon regeneration in the mammalian central nervous system (CNS) has been attributed to the unfavourable tissue microenvironment, i.e. the presence of neurite outgrowth-inhibitory proteins – particularly myelin-associated inhibitors or components of the extracellular matrix (ECM) – in conjunction with lack of axon growth promoting substrates (review: Fawcett, 2006; Busch and Silver, 2007; Lee and Zheng, 2012; Chew et al., 2012).

In the regenerating CNS of fish, amphibians, and reptiles, several putative neurite growth inhibitory proteins and their receptors have been studied (Bastmeyer et al., 1991; Sivron et al., 1994; Lang et al., 1995, 2008; Wanner et al., 1995; Becker et al., 1999, 2004; Klinger et al., 2004a, b; Pesheva et al., 2006; Becker and Becker, 2007). However, the causal relationship between the expression of neurite growth inhibitors and regenerative capacity in these vertebrates remains controversial, and the question whether regeneration of RGC axons is generally facilitated by absence, down-regulation or clearance of inhibitory proteins is unresolved. Down-regulation of proteins known to inhibit axon growth in mammals has been described in the fish (Sivron et al., 1994; Becker et al., 2004) and amphibian (Becker et al., 1999) visual system following optic nerve injury. Other studies failed to detect inhibitory activity in CNS myelin and oligodendrocytes of fish (Bastmeyer et al., 1991; Wanner et al., 1995). In frogs, the presence of axon growth inhibitory properties in spinal cord, but not optic nerve myelin appears to correlate with the lack of regenerative capacity in the spinal cord and regenerative success in the optic pathway (Lang et al., 1995). We demonstrated that the ECM components tenascin-R (TN-R, Pesheva et al., 1993) and chondroitin sulfate proteoglycan (Busch and Silver, 2007), while anti-adhesive and inhibitory to growth of most mammalian axons, are up-regulated in the injured visual pathway and fail to inhibit retinal axon regeneration in the lizard (Lang et al., 2008).

Nogo-A, a member of the reticulon family, is one of the most potent and extensively studied of all neurite growth inhibitory proteins in the mammalian CNS (review: Pernet and Schwab, 2012).

Nogo-A expression is associated with myelin and oligodendrocytes and considered to contribute critically to the failure of CNS axon regeneration in the mature mammalian CNS (Schwab, 2010). Blocking of the function of Nogo-A in the rat has been shown to promote CNS axon regeneration (Schwab, 2010). Inhibition of axon growth and growth cone collapse by Nogo-A are mediated by the glycosylphosphatidylinositol (GPI)-anchored Nogo-A receptor (NgR) on the axonal surface, where it has been shown to form part of a lipid raft-associated receptor complex which includes the low affinity nerve growth factor receptor (p75^{NTR}) and other co-receptors (review: Borrie et al., 2012). This receptor complex also mediates the neurite-growth inhibitory effects of mammalian myelin-associated glycoprotein (MAG) and oligodendrocyte-myelin glycoprotein (OMgp) and is thus thought to play a central role in the signal transduction process underlying axon growth inhibition (Giger et al., 2008; McDonald et al., 2011). As a crucial consequence of activation of the NgR complex, RhoA GTPase is activated and intracellular cyclic adenosine monophosphate (cAMP) levels and thus protein kinase A (pkA) activity are lowered, preventing the dynamic remodeling of the growth cone cytoskeleton required for axon growth or even causing growth cone collapse (review in Peace and Shewan, 2011).

In contrast to mammals, there is a scarcity of data on the expression and function of Nogo-A and NgR in non-mammalian vertebrates. Zebrafish express *rtn4*, which lacks the Nogo-A-specific domain found in mammals and fails to inhibit axon growth (Abdesselem et al., 2009), even though zebrafish possess NgR (Klinger et al., 2004a). Amphibians (*Xenopus*) express Nogo-A (Klinger et al., 2004b), but no data on the functional properties of *Xenopus* Nogo-A are published.

Several species of reptiles, which are amniotes and phylogenetically more closely related to mammals than the other vertebrate classes capable of CNS axon regeneration, have been shown to spontaneously regenerate RGC axons (Rio et al., 1989; Lang et al., 1998; Dunlop et al., 2004).

Thus, analysis of the expression patterns and functions of Nogo-A, its receptor, as well as other proteins relevant to the regenerative process in this vertebrate class is of interest. We have previously shown that RGC axons in the lizard visual system regenerate successfully despite the

persistence of myelin markers (e.g. MBP, PLP) and neurite growth inhibitor antigens revealed by monoclonal antibody IN-1 immunostaining (Caroni and Schwab, 1988; 1989; Lang et al., 1998) which recognizes - but is not specific to - Nogo-A (Chen et al., 2000; Lee et al., 2010, Schwab, 2010).

Against this background, we studied the expression pattern and post-injury regulation of Nogo-A and NgR, as well as the role of the cAMP/pkA pathway involved in Nogo-A/NgR signaling, after optic nerve lesion in the lizard (*G. galloti*), by means of immunohistochemical analysis using cross-species specific rabbit pABs raised against the rat homologues of Nogo-A and NgR in conjunction with established immunohistochemical markers of neurons and glial cells. Together with functional studies evaluating axon outgrowth on substrates of recombinant Nogo-A-Fc in combination with the axon growth-promoting substrate, laminin, as well as KT5720-inhibition of pkA activity, our results indicate that Nogo-A and NgR are expressed and possibly contributing to inhibitory substrate properties in the regenerating lizard visual pathway. However, inhibition of lizard RGC axon regeneration by Nogo-A may be overridden in the presence of laminin and an active cAMP/pkA signalling pathway.

MATERIALS AND METHODS

Animals, tissue fixation and embedding

We used 20 fertilized eggs and 25 adult *G. galloti*, a lacertid species indigenous to the island of Tenerife (Spain). They were collected under permit in their natural environment in compliance with local nature conservation legislation (Autonomous Government of the Canary Islands) and maintained and treated in the laboratory according to Spanish animal welfare legislation, with permission from the Animal Research Ethics Committees of the University of Las Palmas de Gran Canaria and the University of Cape Town. Embryonic development stages were defined according to the tables of *Lacerta vivipara* (Dufaure and Hubert, 1961). Adult animals were kept in large holding tanks fitted with overhead infrared heaters and lighting (light/dark cycles of 12h, temperature during light cycle c. 25°C). Animals had free access to water and a mixed diet of commercially available cat food, cereals, as well as a variety of fruits. Adult lizards were anesthetized by intraperitoneal injection with Diazepam 12.5mg/kg + ketamine 250mg/kg before transcardial perfusion (4% paraformaldehyde or Bouin's fixative). Embryos brains were dissected and immersed in the same fixatives for 6 h. Paraformaldehyde-fixed brains were then cryoprotected in 30% sucrose-PBS overnight, embedded in Tissue-tek®, frozen at -80°C to be finally cut at 14 µm thick in the horizontal or transversal plane in a Reichert-Jung cryostat. Bouin-fixed brains were embedded in paraffin and cut at 10 µm.

Ten neonate (P0-P3) and ten adult Sprague Dawley rats (150g) were obtained from the animal facility of the University of Las Palmas de Gran Canaria. They were anesthetized by intraperitoneal injection with ketamine 80 mg/kg + xylazine 5 mg/kg before optic nerve lesions or preparation of retina (adult rats) and dorsal root ganglion (DRG) explant cultures (neonates).

Unilateral lizard and rat optic nerve lesions

The lizards were anesthetized as described above and maintained on ice to minimise bleeding during surgery. An incision was made along the margin of the largest supraocular osteodermal

plaque, to expose the optic nerve. The right nerve was transected about 1 mm from the eye using iridectomy scissors, and care was taken not to injure the blood vessels supplying the retina. For purposes of orientation, the term “proximal” in the text refers to the portion of the optic nerve between the optic nerve head and the lesion site. Following optic nerve lesion, the osteodermal plaque was put back in place and the lizards returned to their holding tanks and monitored. The animals behaved and fed normally after recovery from anaesthesia. They were left to recover over various time intervals and at least 3 animals were examined at each individual time point (1, 3, 6, and 12 months following optic nerve transection).

Unilateral optic nerve crush lesions in rats were carried out intraorbitally according to established protocols and the animals left to recover for 10 days, the established optimal time point of RGC response (Ford-Holevinski et al., 1986), before terminal anesthesia and dissection of the retinas.

Antibody characterization

Table 1 provides a summary of the primary antibodies used in this study. The rabbit polyclonal anti-Nogo-A antibody (Biotrend - Alpha diagnostic International -, Germany) was raised against rat Nogo-A. It recognizes a protein band of an apparent molecular weight of around 200 kDa in rat and *G. galloti* brain extracts and the staining pattern in *G. galloti* (present study) resembles that observed in the mammalian CNS (Chen et al., 2000). A mouse monoclonal antibody to Nogo-A (clone 11C7, kind gift of M. Schwab, Zurich, Switzerland, RRID: AB_10000211; Pernet et al., 2008), gave similar results (not shown in this study).

The rabbit polyclonal anti-Nogo-66 receptor (NgR) antibody (Biotrend/Alpha Diagnostic International, Germany, RRID: AB_1620281) was raised against human NgR peptide. It recognizes a single protein band of an apparent molecular weight of around 75 kDa in both, rat and *G. galloti* brain extracts (present study).

The rabbit polyclonal anti-cAMP antibody (Sigma-Aldrich, St. Louis, MO, RRID: AB_257899) was raised against 3'5'cAMP-2' - conjugated to bovine serum albumin. Our staining pattern (see

Results) matched the previously published pattern shown by Rodger et al. (2005) in the goldfish retina.

Tuj1 (R&D Systems, Wiesbaden-Nordenstadt, Germany, RRID: AB_357520) is a mouse monoclonal antibody raised against rat microtubules. In the immunoblots, Tuj1 recognizes a single protein band of an apparent molecular weight of around 47 kDa in *G. galloti* brain extracts (Romero-Alemán et al., 2010). Tuj1 showed a neuron specific labeling in the developing and regenerating lizard CNS (Romero-Alemán et al., 2010, 2012).

SMI-31 (Sternberger Monoclonals, Baltimore, MD, RRID: AB_2314901) is a mouse monoclonal antibody raised against phosphorylated neurofilaments (NF) isolated from homogenized rat hypothalami. It stains neurofilaments in *G. galloti* visual system (Lang et al., 1998, 2002; Santos et al., 2011). Moreover, it recognizes two protein bands of about 200, 160 kDa in *G. galloti* brain extracts (Santos et al., 2011) which are according to the NF-H and NF-M isoforms in mouse brain (Xiao and Monteiro, 1994).

The rabbit polyclonal anti-PLP antibody (kind gift of Dr C. Linington, Martinsried, Germany) was raised against rat PLP. In *G. galloti* visual system, it has been previously used to stain myelin sheaths (Lang et al., 1998) and yielding a similar staining pattern as a mouse monoclonal anti-PLP/DM20 antibody (Serotec) also used in this lab (Santos et al., 2006).

Rat monoclonal anti-MBP, clone 6B1 (supernatant) was raised against guinea pig MBP (kind gift of Dr C. Linington, Martinsried, Germany). This antibody has been previously used to stain myelinated structures in *G. galloti* (Lang et al., 1998; Romero-Alemán et al., 2003; Santos et al., 2006).

Mouse monoclonal anti-O4 (kind gift of Dr P. Pesheva, Bonn, Germany, RRID: AB_2619717) is specific for sulfated glycolipids of bovine myelin and has been used previously in several studies of myelin-forming cells in fish (Wanner et al., 1995), amphibians (Lang et al., 1995), and reptiles (Lang et al., 1998).

Mouse monoclonal anti-GFAP antibody (Sigma-Aldrich, St. Louis, MO, RRID: AB_477010) is raised against GFAP preparations from porcine spinal cord. Its specificity in lizard brain has been confirmed by the detection of a single band of around 51-55 kDa in a Western blot analyses (Casañas et al., 2011; Santos et al., 2011) and by astroglia specific staining pattern (Monzón-Mayor et al., 1990; Lang et al., 2002, 2008; Romero-Alemán et al., 2003, 2004; Santos et al., 2008). This antibody has been extensively used to stain astroglial cells in *G. galloti* CNS (Monzón-Mayor et al., 1990; Romero-Alemán et al., 2003, 2004; Lang et al., 2002, 2008; Casañas et al., 2011; Santos et al., 2011).

The rabbit polyclonal anti-p75 neurotrophin receptor (p75^{NTR}, Millipore/Chemicon, Germany, RRID: AB_11211656) was raised against mouse p75^{NTR}. This antibody recognizes a band of approx. 75 kDa in Western blots of lizard brain homogenate (not shown), consistent with p75^{NTR} protein.

Axonal tracing

For anterograde tracing of regenerating lizard RGC axons (Lang et al., 2002), 1 µl of a 10% (w/v) solution of horseradish peroxidase (HRP; type VI, Sigma-Aldrich St. Louis, MO) in phosphate-buffered saline (PBS) containing 1% Triton-X-100 was injected into the right eye of anesthetized control and experimental lizards at various timepoints after optic nerve lesion. Following the HRP injections, animals were allowed to recover for 4 d. Then, the brains were dissected and processed for immunofluorescence detection of HRP using a mouse monoclonal anti-peroxidase antibody (Sigma-Aldrich St. Louis, MO).

Cell and tissue culture

For preparation of homogenous substrates, nitric acid-cleaned glass coverslips were incubated (1 hour, 37°C) with 50 µg/ml poly-L-lysine (Sigma-Aldrich, Seelze, Germany) in ddH₂O. After thorough rinsing in ddH₂O, coverslips were incubated (1 hour, 37°C) with the following proteins or

mixtures in PBS: recombinant Nogo-A-Fc chimera peptide containing amino acids 544-725 of rat Nogo-A (R&D Systems, Inc, 2-8 $\mu\text{g/ml}$) or laminin from EHS sarcoma (Sigma-Aldrich, 20 $\mu\text{g/ml}$). For choice assays, stripes of Nogo-A-Fc (5 $\mu\text{g/ml}$) were applied onto poly-L-lysine-coated coverslips using striped silicone matrices (kindly provided by S. Lang, Max Planck Institute of Developmental Biology, Tuebingen, Germany) for 1 hour at 37°C. The coverslips were then rinsed with PBS and incubated with laminin (20 $\mu\text{g/ml}$) for 1 hour at 37°C. Following coating with substrate proteins, coverslips were rinsed in medium and immediately used for cell and tissue culture. To verify the quality of substrates, some coated coverslips were subjected to immunohistochemical staining for Nogo-A or laminin, which revealed homogeneous distribution of the respective proteins.

Glial cell cultures were prepared by dissociation of lizard brains at embryonic stage 37 (E37) as described previously (Lang et al., 1998). Cells were plated on poly-L-lysine-coated coverslips, the cultures were maintained for 3-7 days at 28°C in the presence of 5% CO₂ and subsequently processed for immunofluorescence labeling.

DRG neurons were prepared from neonate rat pups (stages P0-P3). The DRG were dissected in L15 medium (Sigma-Aldrich), freed of connective tissue and nerve roots, and cut into small pieces on a McIlwain tissue chopper. The fragments were resuspended in L15 containing 20% fetal calf serum (Sigma-Aldrich) and passed repeatedly through a Pasteur pipette with a rounded tip to dissociate the tissue mechanically. Remaining tissue aggregates were allowed to settle for 5 minutes, the suspended cells were centrifuged briefly, taken up in DMEM/F12 (1:1) culture medium supplemented with 10% fetal calf serum, 0.4% methyl cellulose, 15 mM HEPES, 50 $\mu\text{g/ml}$ bovine transferrin, 5 $\mu\text{g/ml}$ bovine insulin, 100 μM putrescine, 30 nM sodium selenite, 20 nM progesterone, 15 nM triiodothyronine, and antimicrobial solution (all from Sigma-Aldrich; 1:100), and plated on coated coverslips as described above. The DRG neurons were cultured in a humidified incubator for up to 48 hours, at 37°C in the presence of 5% CO₂.

Lizard and rat retinal explants were prepared from adult animals that had received a conditioning optic nerve lesion between 3-6 months (lizards) and for 10 days (rats) prior to dissection, as described previously (Ford-Holevinski et al., 1986; Lang et al., 1998; 2002). Briefly, the retinae were dissected free from the sclera and flat-mounted with the RGC layer up on nylon filters (Amersham, Madrid, Spain). The retinae were then cut into strips (width 400 μm) on a McIlwain tissue chopper and placed, RGC layer facing down, on coverslips coated with the respective combinations of substrate proteins. The explants were cultured in a humidified incubator for up to 72 hours in DMEM/F12 medium supplemented as above, at 28°C in the presence of 5% CO₂. For functional studies, soluble Nogo-A-Fc protein (final concentration 2-8 $\mu\text{g}/\text{ml}$) and/or the selective pKA inhibitor KT5720 (Sigma-Aldrich, Germany, final concentration 8 μM) were added to the medium of neonate rat DRG and adult lizard retina explant cultures. In some cases, phospholipase C (Sigma-Aldrich, 0.5U/ml) was added to retina explants cultures (1 hour, 28°C) to remove PGI-anchored NgR from axonal surfaces.

Cultures of DRG neurons and retinal explants were observed and photographed using phase-contrast optics at various time points, or fixed and processed for immunohistochemistry and fluorescence microscopy.

Immunohistochemical procedures

Sections of lizard brains were subjected to a multiple immunofluorescence procedure and labeled with appropriate combinations of the following primary antibodies: rabbit polyclonal antibody (pAB) to rat Nogo-A (Biotrend/Alpha diagnostics; 1:1000); rabbit pAB to human Nogo-66 receptor (NgR, Biotrend/Alpha Diagnostics; 1:1000), rabbit pAB to the p75^{NTR} (Millipore/Chemicon; 1:200), rabbit pAB to rat proteolipid protein (PLP, gift of Dr. C. Linington, Martinsried, Germany; 1:1000), rat monoclonal antibody (mAB) to guinea pig myelin basic protein (MBP, clone 6B1, gift of Dr. C. Linington, Martinsried, Germany; 1:10), mouse mAB to neurofilaments (NF, Sternberger Monoclonals; 1:1000), mouse mAB to neuron-specific betaIII-

tubulin (Tuj-1, R&D systems, Germany; 1:500), mouse mAB to GFAP (Sigma-Aldrich; 1:500), rabbit pAB to cAMP (Sigma-Aldrich, Germany; 1:50) and mouse mAB to HRP (Sigma-Aldrich; 1:100). Immunostainings for Tuj1, GFAP, SMI-31, MBP, PLP, O4 in *G. galloti* visual system were performed according to previously established protocols (Lang et al., 1998, 2002; Romero-Alemán et al., 2010; Santos et al., 2011).

Cell surface labeling of living cultures was performed by incubating the cells with the respective primary antibodies (anti-NgR pAB, anti-p75^{NTR} pAB or the oligodendrocyte marker mouse mAB O4 (gift of P.Pesheva, Mainz, Germany; 1:10) diluted in culture medium for 45 minutes at 4°C, followed by rinsing in culture medium, immersion in methanol (5 minutes, -20°C), fixation in 4% PFA in PBS (5 minutes, room temperature). After washing in PBS, the sections or coverslip cultures were blocked in PBS containing 1% bovine serum albumin and subsequently incubated (overnight at 4°C) with combinations of the respective primary antibodies. Bound primary antibodies were visualized by incubation (2 hours at room temperature) with combinations of the appropriate secondary antibodies: donkey-anti-mouse, donkey-anti-rabbit or donkey anti-rat-Cy3 (Jackson ImmunoResearch Laboratories, USA; 1:1000), and goat-anti-mouse or goat-anti-rabbit-Alexa 488 (Molecular Probes, USA; 1:500). Cell nuclei were counterstained with 4',6'-diamidino-2-phenylindolehydrochloride (DAPI; 0.5 µg/ml in PBS; Sigma-Aldrich) and sections coverslipped in Mowiol (Hoechst, Frankfurt, Germany). Negative controls were treated identically, except for omission of either the primary or the primary and secondary antibodies or, where applicable, incubation with the respective pre-immune sera instead of antisera. No staining above endogenous background levels was detectable in these controls.

Western blot analyses

Brain tissue of adult lizards and rats was homogenized on ice in lysis buffer (20 mM Tris-HCl pH 8, 137 mM NaCl, 10% glycerol and 1% Triton X-100) containing protease inhibitors. The protein

content of the tissue extracts was determined according to Bradford's method. SDS-PAGE was carried out on 10% gels under reducing conditions and separated proteins were electroblotted to nitrocellulose membranes (Hybond ECL, Amersham). The membranes were blocked for 1 h in TBS (20 mM Tris-HCl, 150 mM NaCl, pH 7) containing 5% skim milk, followed by incubation with rabbit polyclonal antibodies (pABs) specific to rat Nogo-A (Biotrend/Alpha Diagnostics, 1:5000) or Human Nogo-A receptor (NgR, Biotrend/Alpha Diagnostics, 1:1000) overnight at 4°C. Binding of the primary antibody was visualized using an anti-rabbit HRP-conjugated secondary antibody (Jackson; 1:50000), followed by enhanced chemiluminescence detection (ECL; Pierce). Controls for antibody specificity included omission of primary antibodies, as well as pre-adsorption of primary antibodies with the corresponding control peptide: NgR control peptide (Biotrend/Alpha Diagnostics, Cat # Ngr11-P); Nogo-A control peptide (Biotrend/Alpha Diagnostics, Cat # AG348). The specificity of the mouse mABs Tuj-1, GFAP and SMI-31 was previously tested by recognition of specific protein bands in western blots of *G. galloti* brain tissue (Romero-Alemán et al., 2010; Casañas et al., 2011; Santos et al., 2011).

Image acquisition and analysis

Acquisition of time-lapse sequences, phase contrast and some immunofluorescence images was carried out on a Zeiss Axiovert 200Mot microscope equipped with Plan-Neofluar objectives. Images were acquired with an AxioCam high resolution monochromatic CCD camera, controlled by Zeiss Axiovision software (V4.6, RRID: SCR_002677). Time lapse recordings were performed in a climate-controlled room for periods up to 48 h, without any noticeable signs of degeneration of the cultures under observation. The majority of immunofluorescence data were acquired using a Zeiss LSM 510 Meta confocal microscope, using the tile scan feature to obtain overview images and optical sectioning for acquisition of z-stacks and creation of maximum intensity projection images. Potential signal crosstalk in multiple immunofluorescence specimens was controlled by

using a multi-track scanning configuration and verifying channel selectivity by scanning single-labeled specimens.

Images were imported into Adobe Photoshop (RRID: SCR_002078) for editing and assembly. In those cases where contrast and brightness values were adjusted, images from intact (unlesioned) tissue were treated identically to those from the lesioned optic pathway.

Quantification of cAMP immunostaining intensity and statistical analysis

Intensity of immunofluorescence labeling for cAMP was quantified post-acquisition on sets of images that had been acquired from sections of identical thickness under identical exposure times and conditions for controls and regenerating tissues. Exposure times were generally shorter than 5 s at 5% laser power, and no detectable photobleaching occurred during image acquisition - as verified by repeatedly taking images of the same areas of interest and measuring their labeling intensities, which resulted in near-identical values. Using the histogram function of the Zeiss AIM confocal software, at least 3 sections per animal were analysed, and a minimum of 3 measurements of areas covering 512 x 512 pixel each were taken per retina section, using a x40 objective. The mean pixel intensities, expressed as greyscale values proprietary to the Zeiss Axiovision software, were pooled for each region of interest in unlesioned control specimens, the intact side in the optic pathway of lesioned animals, and the lesioned optic pathway. The same measurement procedure was carried out on negative control sections where the respective primary antibodies had been omitted, and the so obtained mean baseline intensity value was subtracted from the mean values of the immunolabeled specimens. Statistical analysis of the raw data was performed with Stat Plus software (AnalystSoft, Inc) using One-Way ANOVA. The level of significance was set at $p \leq 0.05$.

RESULTS

Nogo-A and NgR are expressed in a mammalian-like pattern in the developing and adult lizard nervous system

We verified specificity of the Nogo-A and NgR antibodies used in this study by Western blot analysis (Fig. 1A). In immunoblots Nogo-A antibodies labeled a broad protein band in the lizard brain extract, corresponding to the approximate molecular weight of 200 kDa seen in the rat brain extracts (Fig. 1A). In addition, a lower molecular weight band was apparent at around 50 kDa, which did not correspond to any known isoform of Nogo. Both bands were abolished by pre-incubation of Nogo-A pAB with the immunising peptide (Fig. 1A), indicating specificity of Nogo-A pAB and that the 50 kDa band represented a degradation fragment of Nogo-A. NgR pAB labeled a specific band at around 75 kDa in both the lizard and rat brain extracts (Fig. 1A). No signal was detected after pre-incubation of NgR pAB with the immunising peptide and upon omission of the primary antibody (Fig. 1A).

Nogo-A in the developing lizard visual pathway (Figs. 1B-D2), was detected in RGC somata and processes in the retina (Figs. 1B, B2), optic tract (Figs. 1C-C2) and retinorecipient layers in the optic tectum (Figs. 1D-D2). The neuronal identity of the labelled structures was confirmed by counterstaining with the neuronal marker Tuj-1. Nogo-A⁺ myelinated axons (as demonstrated by double-labelling with anti-MBP antibodies) were observed in the optic tract, adjacent to Nogo-A⁺ unmyelinated axons of the hypothalamus at hatching (Figs. 1C-C2). Outside the visual system, Nogo-A immunoreactivity was prominent in brain stem nuclei (Figs. 1F, F1) and DRG neurons (Figs. 1E, E1) of the developing and adult lizard. In the adult CNS, a shift of Nogo-A expression to oligodendrocyte cell bodies and myelin was evident, shown by colocalization with the CNS myelin protein, PLP, in myelinated axons (Figs. 1G-G2) and mature oligodendrocyte somata, which demonstrate cytoplasmic localization of Nogo-A (Figs. 1H-H2). Expression of Nogo-A was also demonstrated in O4-positive lizard oligodendrocytes *in vitro* (Figs. 1I, I1). However, Nogo-A labelling was absent from astrocytes, identified by expression of GFAP (Figs. 1I2, I3).

NgR immunoreactivity in the developing visual pathway (Figs. J-M2) was prominent in RGC axons in the retinal nerve fiber layer (Figs. 1J-K1), optic nerve (Figs. 1K,K1) and the retinorecipient layers of the superficial optic tectum (Figs. 1L-M2), identified by counterstaining with Tuj-1, during stages E32-E39. NgR labeling of retinal axons declined at later stages of development (not shown). In adult animals and in the contralateral (intact) side of lizards after optic nerve lesion, NgR expression was low along the visual pathway (e.g. see intact retina and optic nerve in Figs. 2C, E).

Nogo-A and NgR are up-regulated after optic nerve injury in the lizard

We further studied the changes of Nogo-A and NgR expression in the regenerating lizard optic pathway. The time course of RGC axon regeneration in *G. galloti* after optic nerve transection has been established previously (Lang et al., 1998, 2002). Thus, we carried out an immunohistochemical analysis of Nogo-A and NgR expression at time intervals between 2 months (when RGC axons begin to cross the lesion site) and 6-12 months after optic nerve lesion (when the regrowing axons reach the optic tectum). After unilateral ON injury, Nogo-A and NgR labeling in the contralateral (intact) visual pathway showed staining patterns similar to those in the control (unlesioned) animals. Our previous findings regarding several neuron and glial markers, among them GFAP, MBP, PLP, S-100, and neurofilaments (Romero-Alemán et al., 2010; Santos et al., 2008; 2011; Casañas et al., 2011), also showed unchanged expression levels in the unlesioned side of the visual pathway. Thus, we considered the intact side of lesioned animals as valid representation of the control conditions. Due to space constraints, only the most relevant changes and timepoints are depicted in the figures.

No significant change of Nogo-A expression was observed in the experimental retina after optic nerve lesion compared to that in the contralateral and control retina (not shown). In the proximal portion of the injured optic nerve and at the lesion site, Nogo-A immunoreactivity remained undetected throughout the observation period, together with the myelin marker PLP (shown here

for 3 months post optic nerve lesion, Fig. 2A, A1). Distal to the lesion site, Nogo-A expression persisted, in line with PLP immunoreactivity (Fig. 2A, A1). At 6 months post lesion, abundant bundles of NF-positive regenerating RGC axons (Fig. 2B) were identified in the Nogo-A immunoreactive optic tract (Fig. 2B1, B2). No further changes in the expression pattern of Nogo-A in the regenerating visual pathway were obvious throughout the remainder of the observation period up to 12 months (not shown).

NgR expression appeared elevated in regrowing RGC axons over the intact contralateral side (Fig. 2C-E), throughout the entire observation period. At 3 months post lesion, Tuj-1- and NgR-positive regenerating RGC axons crossed the lesion site (Fig. 2E-F2). To confirm that NgR-labelled structures were indeed newly regenerated axons, we carried out HRP-tracing experiments on lizard optic nerves after various times post lesion. Double-labeling of HRP anterogradely transported in axons and NgR immunostaining resulted in signal colocalization (Fig. 2G-G2), indicating that the NgR-positive structures were indeed regenerated RGC axons. Thus, down-regulation of Nogo-A, or its receptor NgR is unlikely to account for the success of RGC axon regeneration in the lizard.

A further possibility we considered was that NgR may not be localised on the cell surface of growth cones during RGC regeneration in lizards, which might render the axons insensitive to the presence of Nogo-A. We stained live *in vitro* regenerating lizard RGC axons with NgR antibodies, avoiding permeabilization of the growth cones, yet NgR immunoreactivity remained detectable (Fig. 2H, H1). Our observations for the NgR co-receptor p75^{NTR} (Fig. 2I, I1) were similar, indicating that NgR and p75^{NTR} are localised on the surface of regenerating growth cones.

Moreover, treatment with phospholipase C abolished NgR immunoreactivity from axonal surfaces *in vitro* (Fig. 2H2, H3), further confirming the specificity of the NgR pAB for the GPI-anchored NgR in the lizard.

Lizard RGC axons are less sensitive to Nogo-A than mammalian axons

Our immunohistochemical data indicate that, unlike most mammalian neurons, lizard RGCs can regenerate their axons through a microenvironment containing Nogo-A. To analyse the effect of Nogo-A on lizard RGC axon growth, we compared the outgrowth of lizard RGC and neonate rat DRG neurites on defined substrates of the growth promoting extracellular matrix protein, laminin, and recombinant Nogo-A-Fc after 2 days *in vitro*. Rat DRG neurites grew profusely on laminin (67 out of 100 analyzed neurons had at least one neurite; three independent experiments; Fig. 3A), but failed to extend on Nogo-A-Fc (92 out of 100 cells had no neurites; Fig. 3C). The presence of Nogo-A-Fc also abolished outgrowth of rat DRG neurites on laminin (76 out of 100 cells had no neurites; Fig. 3B), confirming the reported inhibitory properties of Nogo-A-Fc for mammalian axons (Chen et al., 2000). In contrast, the outgrowth of RGC neurites from lizard retinal explants was not impeded on a combined substrate of laminin and Nogo-A-Fc (Fig. 3E) compared to laminin alone (Fig. 3D). Lizard RGC neurites grew vigorously even on Nogo-A-Fc (Fig. 3F) and the only noticeable, qualitative difference in the outgrowth pattern was a greater extent of fasciculation and shorter axon length. In all of the above instances, lizard RGC axons covered more than 1% of the substrate area in the acquired images (46 frames in total, representing three independent experiments).

Nogo-A is known to mediate axon growth inhibition by inducing collapse of growth cones. We carried out time lapse assays to study the response of individual lizard RGC growth cones in the presence of soluble Nogo-A-Fc. Upon addition of 2 $\mu\text{g/ml}$ Nogo-A-Fc, collapse was observed in only 21% of analysed growth cones (Fig. 4C), and growth cone morphology and extension typically remained unchanged (Fig. 4B). This result was not different to that obtained in the absence of Nogo-A-Fc (Fig. 4C), indicating that Nogo-A-Fc failed to induce collapse of lizard RGC growth cones over and above the spontaneously occurring collapse frequency. The outcome remained unchanged when testing higher concentrations of Nogo-A-Fc (up to 8 $\mu\text{g/ml}$, data not

shown). Nogo-A-Fc did, however, induce collapse of 82% of rat DRG growth cones (Fig. 4C) and typically caused subsequent neurite retraction (Fig. 4A).

These data indicate that Nogo-A-Fc, as a substrate or in soluble form, does not exert an inhibitory influence on lizard RGC axons growing *in vitro*, thus supporting and partially explaining our findings of successful retinal axon regeneration in the lizard.

Blocking of the pkA signaling pathway renders Nogo-A inhibitory to lizard RGC axons

The activity of the pkA signaling pathway is regulated by intracellular cAMP levels which is critically involved in the ability of axotomized mammalian neurons to regenerate their axons through the inhibitory CNS microenvironment (Hannila and Filbin, 2007). Using the specific pkA inhibitor, KT5720, we evaluated whether pkA signaling is required for regeneration of lizard RGC axons. Addition of 8 μ M of KT5720 failed to prevent axon outgrowth from lizard retinal explants *in vitro* on laminin and on mixed substrates of laminin and Nogo-A-Fc (Fig. 3G,H). However, few or no axons extended in the presence of KT5720 on Nogo-A-Fc when offered as a sole substrate (Consistently less than 1% coverage of the substrate area by axons in the acquired 12 images, representing three independent experiments; Fig. 3I). This stands in marked contrast to the observation of profuse lizard RGC axon growth on Nogo-A-Fc in the absence of the pkA inhibitor (Fig. 3F). Thus, lizard RGC axons require a functional pkA signaling pathway to utilize Nogo-A as a growth substrate. However, the presence of the axon growth promoting substrate, laminin offsets the lack of pkA signaling and allows the axons to extend. We also studied responses of individual lizard RGC growth cones to Nogo-A-Fc in the presence of KT5720 in a series of time-lapse experiments. Addition of up to 8 μ M KT5720 did not affect growth cone morphology and elongation velocity on substrates of laminin or a combination of laminin and Nogo-A-Fc (Fig. 5A, D). On Nogo-A-Fc as sole substrate, KT5720 caused axon retraction (Fig. 5B, D). Unexpectedly, however, this effect was not caused by a significant increase of growth cone collapse events, but rather due to shortening and retraction of axon shafts, while growth cones typically remained

spread out and motile (Fig. 5C). These results confirm that growth of lizard RGC axons is not affected by blocking pKA activity in the presence of laminin, indicating that the outgrowth promoting action of this substrate might not depend on pKA signaling. Axon growth on Nogo-A-Fc, on the other hand, is sensitive to inhibition of pKA signaling, but this effect is not mediated or accompanied by growth cone collapse.

Because pKA signaling appears necessary for growth of lizard RGC axons on Nogo-A-Fc, and it is known that intracellular cAMP levels govern pKA activity, we hypothesized that cAMP levels in axotomized lizard RGC neurons might be higher than those in their mammalian counterparts, which do not regenerate spontaneously. We detected and quantified cAMP immunohistochemically in axotomized lizard and rat RGCs at the height of their regenerative response (3 months and 10 days post optic nerve lesion, respectively). Indeed, lizard RGCs from the lesioned side showed a significant increase of cAMP immunofluorescence signal compared to the intact side, or to rat RGCs after optic nerve lesion (Fig. 6A-D). This increase is sustained during the entire observation interval up to 12 month post lesion (Fig. 6D). Increased cAMP staining is also detectable in regenerating lizard RGC axons in the optic pathway (Fig. 2J-J1) and in lizard RGC growth cones *in vitro* (Fig. 2K-K1). Thus, lesion-induced increase of cAMP levels, and hence increased pKA activation, are likely to facilitate axon regeneration of lizard RGCs *in vivo*.

The above results consistently demonstrate that Nogo-A-Fc fails to inhibit growth of lizard RGC axons, except as a sole substrate and in the absence of pKA signaling. While these observations are striking when compared to findings in mammals, it is obvious that extending growth cones are not likely to encounter homogeneous substrates *in vivo*. We therefore asked whether confrontation of lizard RGC axons with Nogo-A-Fc substrate boundaries might be able to steer growth cones. On substrates consisting of alternating stripes of laminin and laminin with Nogo-A-Fc, lizard RGC axons grew without regard to the substrate boundaries (10 out of 12 evaluated retinal explants, no outgrowth observed in 2 explants from 3 independent experiments; typical result shown in Fig. 7A). In the presence of KT5720, however, the axons grew confined to those stripes containing

laminin only (7 out of 12 retinal explants, no outgrowth observed in 5 explants from 3 independent experiments; typical result shown in Fig. 7B). These data suggest that cAMP-mediated regulation of pKA activity might provide a means to utilize boundaries of Nogo-A distribution as a guidance cue during RGC axon growth and regeneration in the lizard.

Accepted Article

DISCUSSION

In the present study, we provide evidence that the putative neurite growth inhibitor, Nogo-A, is expressed in the lizard, *G. galloti*, in a pattern resembling that seen in the mammalian CNS. The similarities in the expression pattern of Nogo-A in mammals and the lizard *G. Galloti* also extend to a shift from predominantly neuronal expression during embryogenesis, to oligodendrocytes and myelin in the maturing animal (Schwab, 2010). In cell somata, Nogo-A immunoreactivity was most prominent within the cytoplasm, consistent with the association of Nogo-A (a member of the reticulon family of proteins) with the endoplasmic reticulum described in mammals (Schwab, 2010). Based on the present immunohistochemical and western blot data, the observation that mAb IN-1, initially raised against an inhibitory fraction of mammalian CNS myelin (Chen et al., 2000) labels virtually identical structures in the lizard CNS (Lang et al., 1998), and taking into account the relatively close phylogenetic proximity of reptiles to mammals, it seems reasonable to assume that the protein detected in the lizard is indeed the lizard homologue of mammalian Nogo-A.

The fact that we found reactivity of a pAB raised against mammalian NgR1 in lizard neurons and detected the appropriate bands in western blots also makes us confident that we actually detected this protein in the lizard. This is further supported by the observation that NgR immunoreactivity could be removed from lizard RGC axons *in vitro* by enzymatic cleavage of GPI-anchors with phospholipase C (present study). However, our results differ substantially from studies of the expression of NgR in the injured mammalian visual pathway (Hunt et al., 2002a,b; Barrette et al., 2007), in that we observed a distinct and sustained increase of NgR immunoreactivity in axotomised RGCs.

Surprisingly, retinal axon regeneration occurs in the presence of Nogo-A and this is accompanied by up-regulation of NgR in the lizard. It is now well established that Nogo-A and NgR homologues are also expressed in the CNS of other vertebrates (zebrafish: Klinger et al., 2004; Welte et al., 2015; axolotl: Hui et al, 2013) that are capable of spontaneous axon regeneration. These data and our current analysis do not support the hypothesis that down-regulation of Nogo-A and/or lack of

expression of its receptor is a prerequisite for axon regeneration in the optic pathway of the lizard or other vertebrates capable of CNS regeneration. To the contrary, there are indications that cell-autonomous neuronal expression of Nogo-A or its homologues may even be required for the regenerative response of RGC axons in rat (Pernet et al., 2012) or zebrafish (Welte et al., 2015).

This appears consistent with our finding of Nogo-A expression in lizard RGCs during development of the visual pathway. However, we did not observe up-regulation of Nogo-A in RGCs during axon regeneration in the adult lizard, but persisting or increased expression of Nogo A in myelin and oligodendrocytes which, in mammals, contributes to poor CNS axon regeneration.

We also determined that p75^{NTR}, one of the co-receptors required for NgR signaling in mammals (McDonald et al., 2011), is co-expressed in regenerating lizard RGC axons. However, there are indications that signalling of the GPI-anchored NgR is mediated and regulated by dynamic association with lipid rafts of the plasma membrane (Giger et al., 2008), and we could not determine in the current study whether the spatiotemporal localisation of NgR with these signaling platforms, and thus its activation, in the lizard is similar to that in mammalian neurons. We also have no data on the expression of another mammalian Nogo-A receptor, PirB (Atwal et al., 2008; Llorens et al., 2011), or the Nogo-66 co-receptor Lingo (Mi et al., 2004) in the lizard.

Notwithstanding these open questions, our functional studies have uncovered substantial differences in the manner regenerating lizard RGC axons respond to recombinant Nogo-A-Fc, when compared to mammalian neurons. Most striking were the observations that Nogo-A-Fc failed to induce growth cone collapse and was a permissive substrate for lizard RGC axon growth. A shortcoming of our study is that native lizard Nogo-A protein was not available. Moreover, it has to be kept in mind that the Nogo-A-Fc construct we used does not contain the full Nogo-A aminoacidic sequence, and most notably lacks the Nogo-66 loop shown to induce growth cone collapse mediated by NgR (McDonald et al., 2011). However, the fact that this construct elicited a robust growth cone collapse and neurite retraction in rat DRG argues for the functional significance of our observations.

Our present data suggest that the intrinsic properties of axotomised lizard RGCs hold the key to their striking response to Nogo-A-Fc, mammalian myelin (Lang et al, 1998) and their ability to regenerate axons. We could show that cAMP levels in lizard RGCs, known to regulate the activity of pkA and cause changes in gene expression patterns through binding of cAMP response element in cell bodies (Peace and Shewan, 2011), are significantly elevated after optic nerve lesion. In mammals, cAMP levels in CNS neurons decrease after embryogenesis, concomitant with a decrease in capacity for axon regeneration and failure to restore high levels of cAMP required for axon regrowth after injury (Peace and Shewan, 2011). Our results are consistent with published findings indicating that artificially raising cAMP levels in mammalian CNS neurons increases their ability to regenerate axons (Schwab, 2010; Peace and Shewan, 2011) and that the cAMP/pkA signaling pathway regulates RGC regeneration in goldfish (Li et al., 2003; Rodger et al., 2005). In keeping with its activation by cAMP, pkA activity proved crucial to growth of lizard RGC axons on Nogo-A-Fc, as demonstrated by the abolition of axon growth on Nogo-A-Fc in the presence of the selective pkA inhibitor, KT5720. Our observation of robust lizard RGC axon growth on Nogo-A-Fc as a sole substrate, on the other hand, could be explained by the elevated cAMP levels of these cells, which, through activation of pkA, might shift the signaling balance in the growth cone towards reduced RhoA activity and thus, reduced sensitivity to the inhibitory effects of neurite growth inhibitors (McDonald et al., 2011). Surprisingly, however, Nogo-A-Fc failed to elicit growth cone collapse even in the presence of KT5720: growth cones maintained motility but simultaneously axon shafts retracted. This could be interpreted to support the notion that the Nogo-66 loop (absent from the Nogo-A-Fc construct we used) is primarily responsible for inducing growth cone collapse (Chivatakarn et al., 2007). Alternatively, the partial sequence of Nogo-A contained in this construct (amino acids 544-725) might exert axon growth inhibition predominantly through non-collapse mechanisms (Schweigreiter et al., 2004). A third possibility is that another, pkA-independent signaling pathway might exist that compensates for the lack of pkA signaling in KT5720-treated lizard RGC growth cones. Indeed, there is mounting evidence for an

important role of the protein kinase C pathway in axon regeneration (Bonnici and Kapfhammer, 2009; Samara et al., 2010; Yang et al., 2010). Finally, it appears likely that the lizard RGC neurons would have been conditioned towards axon regeneration by the optic nerve lesion preceding our *in vivo* regeneration experiments. Thus, transcription-dependent changes in gene expression priming the neurons for axon regrowth might be induced in lizards as reported in other vertebrates (Peace and Shewan, 2011), possibly towards overriding the axon growth inhibitory influence of Nogo-A and other neurite growth inhibitors like TN-R (Lang et al., 2008).

The gene expression changes underlying a conditioning lesion are known to be mediated by cAMP (Hannila and Filbin, 2008). This is supported by our observations that cAMP in lizard RGCs became strongly elevated around 6 weeks after optic nerve lesion, preceding the onset of axon regeneration, and persisted throughout the regenerative period observed. Moreover, a conditioning lesion is necessary to make lizard RGCs competent for axon regeneration, and is sufficient to induce robust axon regeneration *in vivo* (Lang et al., 2002). Thus, it is likely that the cAMP/pKA signaling pathway influences processes directly involved in the RhoA-activity mediated inhibition of cytoskeletal reorganization underlying axon extension, as well as long-term transcriptional changes conditioning the axotomized lizard RGC neurons for axon regrowth. These results also raise the question as to the underlying causes of the significant and sustained elevation of cAMP levels in lizard RGCs after injury. Our previous data suggest at least two possibilities: firstly, neurotrophins are known to promote activity of the cAMP/pKA signaling pathway, thus counteracting the RhoA-mediated inhibition of axon growth. Indeed, up-regulation of neurotrophins has been demonstrated recently in the injured visual pathway of the lizard (Santos et al., 2008; 2011). Secondly, we have demonstrated that axon growth-promoting ECM molecules like laminin and fibronectin are up-regulated after optic nerve lesion in the lizard (Lang et al., 2008), and our present work confirms that the presence of laminin in the substrate offsets any growth inhibition of lizard RGC axons effected by Nogo-A-Fc. Thus, the upregulation of

neurotrophins and axon growth promoting ECM in the lizard may be a crucial difference in the microenvironments of the injured visual pathway in reptiles and mammals.

While the present study clearly demonstrates a lack of inhibition of RGC axon regeneration by Nogo-A, the actual function of this protein in the lizard visual pathway remains essentially unclear.

A possible clue is provided by our choice assays, which unmasked a channeling function exerted by an *in vitro* substrate boundary of Nogo-A-Fc in the presence of the pkA inhibitor KT5720. This could indicate that, depending on the activation status of the pkA signaling pathway, Nogo-A might be involved in the guidance, fasciculation and plasticity of growing axons during development and regeneration (review in Schwab, 2010; Llorens et al., 2011). Our finding that, like in mammals, Nogo-A expression in the lizard changes from a predominantly neuronal pattern during embryogenesis to localization in oligodendrocytes and myelin in the maturing animal, also suggests that there might be a function for Nogo-A during axon growth and neuronal development preceding myelination (Petrinovic et al., 2010) and this is emphasized by the fact that NgR is up-regulated by RGCs during axon growth in lizard embryos.

CONCLUSIONS

We conclude that lizard Nogo-A and NgR are expressed in a pattern similar to that described in mammals and axon regeneration in the lizard optic pathway is successful despite the persisting expression of Nogo-A and the up-regulation of NgR expression by regenerating RGCs. We also demonstrate that recombinant mammalian Nogo-A-Fc fails to inhibit growth of lizard RGC axons and provide a possible explanation of this surprising result by our finding of elevated cAMP levels which may help the damaged lizard RGCs to mount and sustain an efficient regenerative response and thus override the influence of Nogo-A-Fc. This study provides insight into the evolution of the interrelationship between neurite growth inhibitory properties of the CNS tissue microenvironment and the intrinsic properties of axotomised neurons, and it demonstrates that the lizard is an

interesting model for further investigation of the functions of Nogo-A and NgR in CNS development and repair.

Acknowledgements: This work has been supported by grants from the South African Medical Research Council (MRC), the South African National Research Foundation (NRF) and the University of Cape Town Research Council (URC) (to DML), as well as the Spanish Ministry of Education (Research Project BFU2007-67139); the Regional Canary Islands Government (ACIISI, Research Project SolSubC200801000281 and ULPAPD-08/01-4) (to MM-M).

We thank Juan Francisco Arbelo-Galván for his excellent technical assistance.

Conflict of interest statement: All authors hereby declare that there is no identified conflict of interest.

Role of authors: All authors hereby declare that they had full access to all the data in the study and take responsibility for the integrity of the data and the accuracy of the data analysis. Study concept and design: DML; MM-M. Acquisition of data: DML, BD. Analysis and interpretation of data: DML; BD; ES-G; MM-M; MR-A. Drafting of the manuscript: DML; MR-A; MM-M. Critical revision of the manuscript for important intellectual content: DML; MR-A; MM-M. Statistical analysis: DML; BD. Obtained funding: DML; MM-M. Administrative, technical, and material support: ES-G; Juan Francisco Arbelo-Galván. Study supervision: DML; MM-M.

LITERATURE CITED

Abdesselem H, Shypitsyna A, Solis GP, Bodrikov V, Stuermer CA. 2009. No Nogo66- and NgR-mediated inhibition of regenerating axons in the zebrafish optic nerve. *J Neurosci* 29(49):15489-15498.

Atwal JK, Pinkston-Gosse J, Syken J, Stawicki S, Wu Y, Shatz C, Tessier-Lavigne M. 2008. PirB is a functional receptor for myelin inhibitors of axonal regeneration. *Science* 322:967-970.

Baldwin KT, Giger RJ. 2015. Insights into the physiological role of CNS regeneration inhibitors. *Front Mol Neurosci*. 8:23.

Barrette B, Vallières N, Dubé M, Lacroix S. 2007. Expression profile of receptors for myelin-associated inhibitors of axonal regeneration in the intact and injured mouse central nervous system. *Mol Cell Neurosci* 34(4):519-538.

Bastmeyer M, Beckmann M, Schwab ME, Stuermer CA. 1991. Growth of regenerating goldfish axons is inhibited by rat oligodendrocytes and CNS myelin but not but not by goldfish optic nerve tract oligodendrocytelike cells and fish CNS myelin. *J Neurosci* 11:626-640.

Becker CG, Becker T, Meyer RL, Schachner M. 1999. Tenascin-R inhibits the growth of optic fibers in vitro but is rapidly eliminated during nerve regeneration in the salamander *Pleurodeles waltl*. *J Neurosci* 19:813-827.

Becker CG, Becker T. 2007. Growth and pathfinding of regenerating axons in the optic projection of adult fish. *J Neurosci Res* 85(12):2793-2799.

Becker CG, Schweitzer J, Feldner J, Schachner M, Becker T. 2004. Tenascin-R as a repellent guidance molecule for newly growing and regenerating optic axons in adult zebrafish. *Mol Cell Neurosci* 26:376-389.

Bonnici B, Kapfhammer JP. 2009. Modulators of signal transduction pathways can promote axonal regeneration in entorhino-hippocampal slice cultures. *Eur J Pharmacol* 612:35-40.

Borrie SC, Baeumer BE, Bandtlow CE. 2012. The Nogo-66 receptor family in the intact and diseased CNS. *Cell Tissue Res*. 349(1):105-17.

Busch SA, Silver J. 2007. The role of extracellular matrix in CNS regeneration. *Curr Opin Neurobiol* 17:120-127.

Caroni P, Schwab ME. 1988. Antibody against myelin-associated inhibitor of neurite growth neutralizes nonpermissive substrate properties of CNS white matter. *Neuron* 1(1), 85–96.

Caroni P, Schwab ME. 1989. Codistribution of neurite growth inhibitors and oligodendrocytes in rat CNS: appearance follows nerve fiber growth and precedes myelination. *Dev Biol* 136(2):287-95.

Casañas N, Santos E, Yanes C, Romero-Alemán MM, Viñoly R, Alfayate MC and Monzón-Mayor M. 2011. Development of astroglia heterogeneously expressing Pax2, vimentin and GFAP during the ontogeny of the lizard (*Gallotia galloti*) optic pathway: Immunohistochemical and ultrastructural study. *Cell Tissue Res* 345(3):295-311.

Chen MS, Huber AB, van der Haar ME, Frank M, Schnell L, Spillmann AA, Christ F, Schwab ME. 2000. Nogo-A is a myelin-associated neurite outgrowth inhibitor and an antigen for monoclonal antibody IN-1. *Nature* 403:434-439.

Chew DJ, Fawcett JW, Andrews MR. 2012. The challenges of long-distance axon regeneration in the injured CNS. *Prog Brain Res*. 201:253-94.

Chivatakarn O, Kaneko S, He Z, Tessier-Lavigne M, Giger RJ. 2007. The Nogo-66 receptor NgR1 is required only for the acute growth cone-collapsing but not the chronic growth-inhibitory actions of myelin inhibitors. *J Neurosci* 27:7117-7124.

Dufaure JP, Hubert J. 1961. Table de développement du lézard vivipare (*Lacerta vivipara jacquin*). *Arch Anat Microsc Morphol Exp* 50:309-327.

Dunlop SA, Tee LB, Stirling RV, Taylor AL, Runham PB, Barber AB, Kuchling G, Rodger J, Roberts JD, Harvey AR, Beazley LD. 2004. Failure to restore vision after optic nerve regeneration in reptiles: interspecies variation in response to axotomy. *J Comp Neurol* 478:292-305.

Fawcett JW (2006) Overcoming inhibition in the damaged spinal cord. *J Neurotrauma* 23:371-383.

Ford-Holevinski TS, Hopkins JM, McCoy JP, Agranoff BW. 1986. Laminin supports neurite outgrowth from explants of axotomized adult rat retinal neurons. *Dev Brain Res* 28:121-126.

Giger RJ, Venkatesh K, Chivatakarn O, Raiker SJ, Robak L, Hofer T, Lee H, Rader C. 2008. Mechanisms of CNS myelin inhibition: evidence for distinct and neuronal cell type specific receptor systems. *Restor Neurol Neurosci* 26:97-115.

Hannila SS, Filbin MT. 2008. The role of cyclic AMP signaling in promoting axonal regeneration after spinal cord injury. *Exp Neurol* 209(2):321-332.

Hui SP, Monaghan JR, Voss SR, Ghosh S. 2013. Expression pattern of Nogo-A, MAG, and NgR in regenerating urodele spinal cord. *Dev Dyn*. 242(7):847-60.

Hunt D, Coffin R, Anderson P. 2002a. The Nogo receptor, its ligands and axonal regeneration in the spinal cord; A review. *J Neurocytol* 31(2):93-120.

Hunt D, Mason M, Campbell G, Coffin R, Anderson P. 2002b. Nogo receptor mRNA expression in intact and regenerating CNS neurons. *Mol Cell Neurosci* 20(4):537-552.

Klinger M, Diekmann H, Heinz D, Hirsch C, Hannbeck von Hanwehr S, Petrusch B, Oertle T, Schwab ME, Stuermer CA. 2004b. Identification of two NOGO/RTN4 genes and analysis of Nogo-A expression in *Xenopus laevis*. *Mol Cell Neurosci* 25:205-216.

Klinger M, Taylor JS, Oertle T, Schwab ME, Stuermer CA, Diekmann H. 2004a. Identification of Nogo-66 receptor (NgR) and homologous genes in fish. *Mol Biol Evol* 21:76-85.

Lang DM, Romero-Alemán M, Arbelo-Galván J, Stuermer C, Monzón-Mayor M. 2002. Regeneration of retinal axons in the lizard *Gallotia galloti* is not linked to generation of new retinal ganglion cells. *J Neurobiol* 52(4):322-335.

Lang DM, Monzón-Mayor M, Bandtlow CE, Stuermer CA. 1998. Retinal axon regeneration in the lizard *Gallotia galloti* in the presence of CNS myelin and oligodendrocytes. *Glia* 23:61-74.

Lang DM, Monzón-Mayor M, Romero-Alemán MM, Yanes C, Santos E, Pesheva P. 2008. Tenascin-R and axon growth-promoting molecules are up-regulated in the regenerating visual pathway of the lizard (*Gallotia galloti*). *Dev Neurobiol* 68:899-916.

Lang DM, Rubin BP, Schwab ME, Stuermer CA. 1995. CNS myelin and oligodendrocytes of the *Xenopus* spinal cord - but not optic nerve - are nonpermissive for axon growth. *J Neurosci* 15:99-109.

Lee JK, Geoffroy CG, Chan AF, Tolentino KE, Crawford MJ, Leal MA, Kang B, Zheng B. 2010. Assessing spinal axon regeneration and sprouting in Nogo-, MAG-, and OMgp-deficient mice. *Neuron*. 2010 Jun 10;66(5):663-70.

Lee JK, Zheng B. Role of myelin-associated inhibitors in axonal repair after spinal cord injury. 2012. *Exp Neurol*. 235(1):33-42.

Li Y, Irwin N, Yin Y, Lanser M, Benowitz LI. 2003. Axon regeneration in goldfish and rat retinal ganglion cells: differential responsiveness to carbohydrates and cAMP. *J Neurosci* 23:7830-7838.

Llorens F, Gil V, del Rio JA. 2011. Emerging functions of myelin-associated proteins during development, neuronal plasticity, and neurodegeneration. *FASEB J* 25(2):463-475.

McDonald CL, Bandtlow C, Reindl M. 2011. Targeting the Nogo receptor complex in diseases of the central nervous system. *Curr Med Chem* 18:234-244.

Mi S, Lee X, Shao Z, Thill G, Ji B, Relton J, Levesque M, Allaire N, Perrin S, Sands B, Crowell T, Cate RL, McCoy JM, Pepinsky RB. 2004. LINGO-1 is a component of the Nogo-66 receptor/p75 signaling complex. *Nat Neurosci*. 7(3):221-8.

Monzón-Mayor M, Yanes C, James JL, Sturrock R. 1990. An ultrastructural study of the development of astrocytes in the midbrain of the lizard. *J Anat* 170:33-41.

Peace AG, Shewan DA. 2011. New perspectives in cyclic AMP-mediated axon growth and guidance: The emerging epoch of Epac. *Brain Res Bull* 84:280-288.

- Pernet V, Joly S, Christ F, Dimou L, Schwab ME. 2008. Nogo-A and myelin-associated glycoprotein differently regulate oligodendrocyte maturation and myelin formation. *J Neurosci*. 28(29):7435-44.
- Pernet V, Joly S, Dalkara D, Schwarz O, Christ F, Schaffer D, Flannery JG, Schwab ME. 2012. Neuronal Nogo-A upregulation does not contribute to ER stress-associated apoptosis but participates in the regenerative response in the axotomized adult retina. *Cell Death Differ*. 19(7):1096-108.
- Pernet V, Schwab ME. 2012. The role of Nogo-A in axonal plasticity, regrowth and repair. *Cell Tissue Res*. 349(1):97-104.
- Pesheva P, Gennarini G, Goridis C, Schachner M. 1993. The F3/11 cell adhesion molecule mediates the repulsion of neurons by the extracellular matrix glycoprotein J1-160/180. *Neuron* 10:69-82.
- Pesheva P, Probstmeier R, Lang DM, McBride R, Hsu NJ, Gennarini G, Spiess E, Peshev Z. 2006. Early coevolution of adhesive but not antiadhesive tenascin-R ligand-receptor pairs in vertebrates: a phylogenetic study. *Mol Cell Neurosci* 32:366-386.
- Petrinovic MM, Duncan CS, Bourikas D, Weinman O, Montani L, Schroeter A, Maerki D, Sommer L, Stoeckli ET, Schwab ME. 2010. Neuronal Nogo-A regulates neurite fasciculation, branching and extension in the developing nervous system. *Development* 137(15):2539-5250.
- Rio JP, Reperant J, Ward R, Peyrichoux J, Vesselkin N. 1989. A preliminary description of the regeneration of optic nerve fibers in a reptile, *Vipera aspis*. *Brain Res* 479:151-156.
- Rodger J, Goto H, Cui Q, Chen PB, Harvey AR. 2005. cAMP regulates axon outgrowth and guidance during optic nerve regeneration in goldfish. *Mol Cell Neurosci* 30:452-464.
- Romero-Alemán MM, Monzón-Mayor M, Santos E, Lang DM, Yanes C. 2012. Neuronal and glial differentiation during lizard (*Gallotia galloti*) visual system ontogeny. *J Comp Neurol* 520:2163-2184.
- Romero-Alemán MM, Monzón-Mayor M, Santos E, Yanes C. 2010. Expression of neuronal markers, synaptic proteins and glutamine synthetase in the control and regenerating lizard visual system. *J Comp Neurol* 518:4067-4087.

Romero-Alemán MM, Monzón-Mayor M, Yanes C, Lang D. 2004. Radial glial cells, proliferating periventricular cells, and microglia might contribute to successful structural repair in the cerebral cortex of the lizard *Gallotia galloti*. *Experimental Neurology* 57:54-66.

Romero-Alemán MM, Monzón-Mayor M, Yanes C, Arbelo-Galván JF, Lang D, Renau-Piqueras J, Negrín-Martínez C. 2003. S100 Immunoreactive glial cells in the forebrain and midbrain of the lizard *Gallotia galloti* during ontogeny. *J Neurobiol* 57:54-66.

Samara C, Rohde CB, Gilleland CL, Norton S, Haggarty SJ, Yanik MF. 2010. Large-scale in vivo femtosecond laser neurosurgery screen reveals small-molecule enhancer of regeneration. *Proc Natl Acad Sci USA* 107(43):18342-1847.

Santos E, Monzón-Mayor M, Romero-Alemán MM, Yanes C. 2008. Distribution of neurotrophin-3 during the ontogeny and regeneration of the lizard (*Gallotia galloti*) visual system. *Dev Neurobiol* 68:31-44.

Santos E, Romero-Alemán MM, Monzón-Mayor M, Lang DM, Rodger J, Yanes C. 2011. Expression of BDNF and NT-3 during the ontogeny and regeneration of the lacertidian (*Gallotia galloti*) visual system. *Dev Neurobiol* 71:836-853.

Santos E, Yanes CM, Monzón-Mayor M, Romero-Alemán MM. 2006. Peculiar and Typical Oligodendrocytes Are Involved in an Uneven Myelination Pattern during the Ontogeny of the Lizard Visual Pathway. *Journal of Neurobiology*. 66:1115-1124.

Schwab ME. 2010. Functions of Nogo proteins and their receptors in the nervous system. *Nat Rev Neurosci*. 11(12):799-811.

Schweigreiter R, Walmsley AR, Niederöst B, Zimmermann DR, Oertle T, Casademunt E, Frentzel S, Dechant G, Mir A, Bandtlow CE. 2004. Versican V2 and the central inhibitory domain of Nogo-A inhibit neurite growth via p75NTR/NgR-independent pathways that converge at RhoA. *Mol Cell Neurosci* 27(2):163-174.

Sivron T, Schwab ME, Schwartz M. 1994. Presence of growth inhibitors in fish optic nerve myelin: postinjury changes. *J Comp Neurol* 343:237-246.

Wanner M, Lang DM, Bandtlow CE, Schwab ME, Bastmeyer M, Stuermer CA. 1995. Reevaluation of the growth-permissive substrate properties of goldfish optic nerve myelin and myelin proteins. *J Neurosci* 15:7500-7508.

Welte C, Engel S, Stuermer CA. 2015. Upregulation of the zebrafish Nogo-A homologue, Rtn4b, in retinal ganglion cells is functionally involved in axon regeneration. *Neural Dev.* 10:6.

Xiao J, Monteiro MJ. 1994. Identification and characterization of a novel (115 kDa) neurofilament-associated kinase. *J Neurosci* 14:1820–1833.

Yang P, Li ZQ, Song L, Yin YQ. 2010. Protein kinase C regulates neurite outgrowth in spinal cord neurons. *Neurosci Bull* 26(2):117-125.

FIGURE LEGENDS

Figure 1: Expression of Nogo-A and NgR during ontogeny of the lizard nervous system. A:

Western blot analysis in lizard and rat brain extracts using anti-Nogo-A and anti-NgR pABs. Each antibody recognizes a single protein band (arrowheads) at the appropriate apparent molecular weight (200 kDa for Nogo-A; 75 kDa for NgR) in lizard and rat brain. Detection of a putative degradation fragment of Nogo-A (around 50 kDa) in lizard samples is abolished by pre-adsorption of the antibody. **B-B2:** At E34, Nogo-A immunofluorescence is present in RGCs, the NFL and the IPL of the retina (B) as demonstrated by counterstaining with Tuj-1 (B1). At hatching stage, Nogo-A signal is restricted to the NFL (B''). **C-C2:** Nogo-A is detected in myelinated axons of the optic tract and adjacent unmyelinated axons in the hypothalamus (C). (C1) Myelination shown by MBP immunofluorescence, (C2) Signal overlay. **(D, D1):** Nogo-A is prominent in axons of the superficial retinorecipient layers of the optic tectum at stage E34 (D). (D1) Counterstain with Tuj-1, (D2) Signal overlay. **E-F1:** In stage E34 embryos, Nogo-A expression is prominent in the cytoplasm and processes of CNS (brain stem, F) and PNS (dorsal root ganglion, E) neurons, as confirmed by Tuj-1 labeling (F1, E1). The signal associated with nucleoli (arrowheads in E, F) is endogenous fluorescence as also occurs in unstained sections. **G-H2:** In adult lizards, double-labeling with PLP (G) and Nogo-A (G') shows signal co-localization in myelinated axons (G2). PLP⁺ oligodendrocytes (H) display Nogo-A signal enriched in the cytoplasm, indicated by arrowheads in (H1), signal overlay shown in (H2). **I-I3:** O4⁺ lizard oligodendrocytes (I), but not GFAP⁺ astrocytes (I2) express Nogo-A (I1, I3). **J-M'':** During embryonic development, Tuj-1⁺ RGC axons (J1, K1, L1, M1) show distinct NgR labeling in the retinal NFL at stage E34 (J), in the ON (E32, K) and in the superficial and deep layers of the OT (E32 and E39, L and M, respectively). (M2) Signal overlay. Scale bars = 10 μ m in B-B2 and G-I3; 100 μ m in C-D2 and K-M2; 20 μ m in E-F1 and J-J1. GCL, ganglion cell layer; IPL, inner plexiform layer; NFL, nerve fiber layer.

Figure 2: Changes of Nogo-A and NgR expression during regeneration of the lizard visual

pathway. A-A1: PLP (A) and Nogo-A expression (A1) persist in the lizard visual pathway 3 months post injury, with the exception of the lesion site (marked by arrowheads). **B-B2:** At 6 months post injury, NF-positive bundles of regenerating axons (B) are traversing the Nogo-A-immunoreactive (B1) optic tract. (B2) Signal overlay. **C-D1:** NgR staining in RGCs is up-regulated (D) compared to the intact situation (C) after optic nerve injury, accompanied by elevated Tuj-1 immunoreactivity (D1). (C1) DAPI staining, indicating position of RGC nuclei. **E:** NgR is up-regulated in the regenerating optic nerve rostral to the lesion site 3 month post injury when RGC axons begin to traverse the injury site (indicated by arrowheads). **F-F2:** Details of the inset area in (E). NgR-positive regenerating axons (F) are identified by Tuj-1 labeling (F1). (F2) Signal overlay. **G-G2:** NgR up-regulation in regenerating RGC axons in the optic tract (G) is demonstrated by HRP tracing (G1) at 6 months post lesion. (G2) Signal overlay. **H-I1:** Lizard RGC growth cones regenerating *in vitro* express NgR (H) and its co-receptor p75^{NTR} (I). (H2) Phospholipase C treatment abolishes cell surface expression of NgR. (H1, H3, I1) Counterstaining and identification of neuronal structures with anti-NF ABs. **J-J1:** Elevated cAMP staining (J) correlates with increased Tuj-1 immunofluorescence (J1) in regenerating lizard RGC axons distal to the lesion site at 3 months post lesion. **K-K1:** (K) cAMP immunoreactivity in lizard RGC growth cones extending on Nogo-A-Fc substrate *in vitro*, identified by Tuj-1 labeling (K1). (K2) Signal overlay. Scale bars = 500 μ m in A-B2 and E; 10 μ m in C-D1, H-I1 and K-K1; 20 μ m in F-G2 and J-J1.

Figure 3: *In vitro* assays on neurite outgrowth in the presence of Nogo-A-Fc and the protein

kinase A (pkA) inhibitor KT5720 (Typical results shown). Neonate rat DRG neurons (A-C) and lizard retinal explants (D-I) were cultured over 48 hr on substrates of polylysine/laminin (LN), polylysine/laminin with Nogo-A-Fc peptide (LN+NogoFc), or polylysine with Nogo-A-Fc (NogoFc). **A-C:** Rat DRG neurites grow profusely on LN (A), but presence of Nogo-A-Fc abolishes neurite growth on LN (B) and polylysine (C). **D-F:** Growth of lizard RGC axons is

robust on LN (D), but also in presence of Nogo-A-Fc on LN (E) or on polylysine (F). **G-I:**

Addition of KT5720 does not affect growth of lizard RGC axons on LN (G) or on LN with Nogo-A-Fc (H), but prevents axon growth on polylysine in the presence of Nogo-A-Fc (I). Scale bar = 100 μm .

Figure 4: Collapse assay in neonate rat DRG (RDRG) and lizard retinal explants (LRGC) 3

months post-lesion. Explants were cultured on polylysine/laminin (LN), soluble Nogo-A-Fc added to the medium and time series of growth cone responses recorded. Phase contrast images were taken 1 hour before (-1 hr), at the time (0 hr) and 1/2hr, 1hr and 2 hr. after the addition of Nogo-A-Fc. Series (A): Typical collapse and retraction response of rat DRG growth cone after addition of Nogo-A-Fc. Series (B): Typical response of lizard RGC growth cones, which fail to collapse and retract after exposure to Nogo-A-Fc. C: Quantification of growth cone responses. Nogo-A-Fc causes collapse and retraction in rat DRG growth cones (RDRG + NogoFc), but fails to elicit collapse and retraction in lizard RGC axons (LRGC + NogoFc) beyond the spontaneous growth cone retraction rate of lizard RGC axons on polylysine/laminin (LRGC on LN). Asterisk denotes significant difference in the responses of RDRG vs LRGC growth cones in the presence of Nogo-A-Fc. (Chi-Square Test, $p \leq 0.05$). n, number of observed growth cones, derived from two (rat DRG neurons) and three (lizard RGC axons) independent experiments, respectively. Scale bar = 10 μm

Figure 5: Time lapse analysis of the effect of the pKa inhibitor, KT5720 on lizard RGC axon growth *in vitro*. Retinal explants were placed on substrates of polylysine/laminin (LN, series A) or polylysine with Nogo-A-Fc (NogoFc, series B). KT5720 was added at the time point 0 (indicated by black arrowhead) and phase contrast time series were recorded between up to 3 hour before and up to 8 hr after addition of KT5720. Series A: Axons on polylysine/laminin continue to grow after addition of KT5720. Axon growth on polylysine/laminin with Nogo-A-Fc (LN+NogoFc, not shown) is not significantly slower and equally unaffected by KT5720 (quantified in D). Series B:

RGC axons on polylysine with Nogo-A-Fc, retract upon addition of KT5720 (see quantification in D). Series C: Higher magnification detail of growth cones indicated by arrowheads in B. KT5720, while causing axon retraction on Nogo-A-Fc, does not elicit collapse of spread growth cones to a significant extent and growth cone motility is maintained. D: Quantification of axonal length expressed as mean \pm standard deviation (SD). n, number of observed events. Scale bars = 100 μ m in A and B; 10 μ m in C.

Figure 6: Immunohistochemical determination of cAMP levels in lizard and rat RGCs after optic nerve transection. Position of RGC nuclei is indicated by DAPI counterstaining. A-B: At 3 months postlesion, the contralateral (intact) lizard retina shows weak staining (A) whereas intensity of anti-cAMP immunofluorescence increases in the damaged RGCs (B). C: Rat RGCs did not show sustained increase of cAMP levels after 10 days postinjury. Boxes in A-C indicate size of areas used for intensity measurements in D. D: Quantification of cAMP immunofluorescence signal in the RGC layer. Densitometric measurements are represented as grayscale values on an arbitrary scale provided by the image analysis software. Intensities were significantly increased (One-Way ANOVA, $p < 0.05$) in the damaged lizard RGCs throughout the observed regeneration period between 2-12 months postlesion (asterisks), over control-like levels (contralateral/intact side) and over cAMP immunofluorescence levels observed in the rat RGCs 10 days postlesion. Data are representative of three different animals per group. Error bars indicate SEM. Scale bar = 50 μ m. D, days postlesion; Int, contralateral intact retina; M, months postlesion; n, number of measurements.

Figure 7: *In vitro* choice assay of growing axons from lizard retinal explants (Typical results shown). Nogo-A-Fc peptide was applied to polylysine-coated coverslips in a striped pattern and the coverslips overlaid with laminin. Axon outgrowth from lizard retinal explants on this patterned substrate was observed in the absence (A) and presence of the pKA inhibitor, KT5720 (B) in the

medium. **A:** Lizard RGC axons do not distinguish between stripes with (grey) and without Nogo-A-Fc (black) in the absence of KT5720. **B:** In the presence of KT5720, axons become restricted to the stripes free of Nogo-A-Fc (black). Dashed lines delineate the adjacent stripes in the phase contrast image. Presence of Nogo-A-Fc is shown by immunostaining with anti-Nogo-A antibody (grey stripes). Scale bar = 100 μm .

Accepted Article

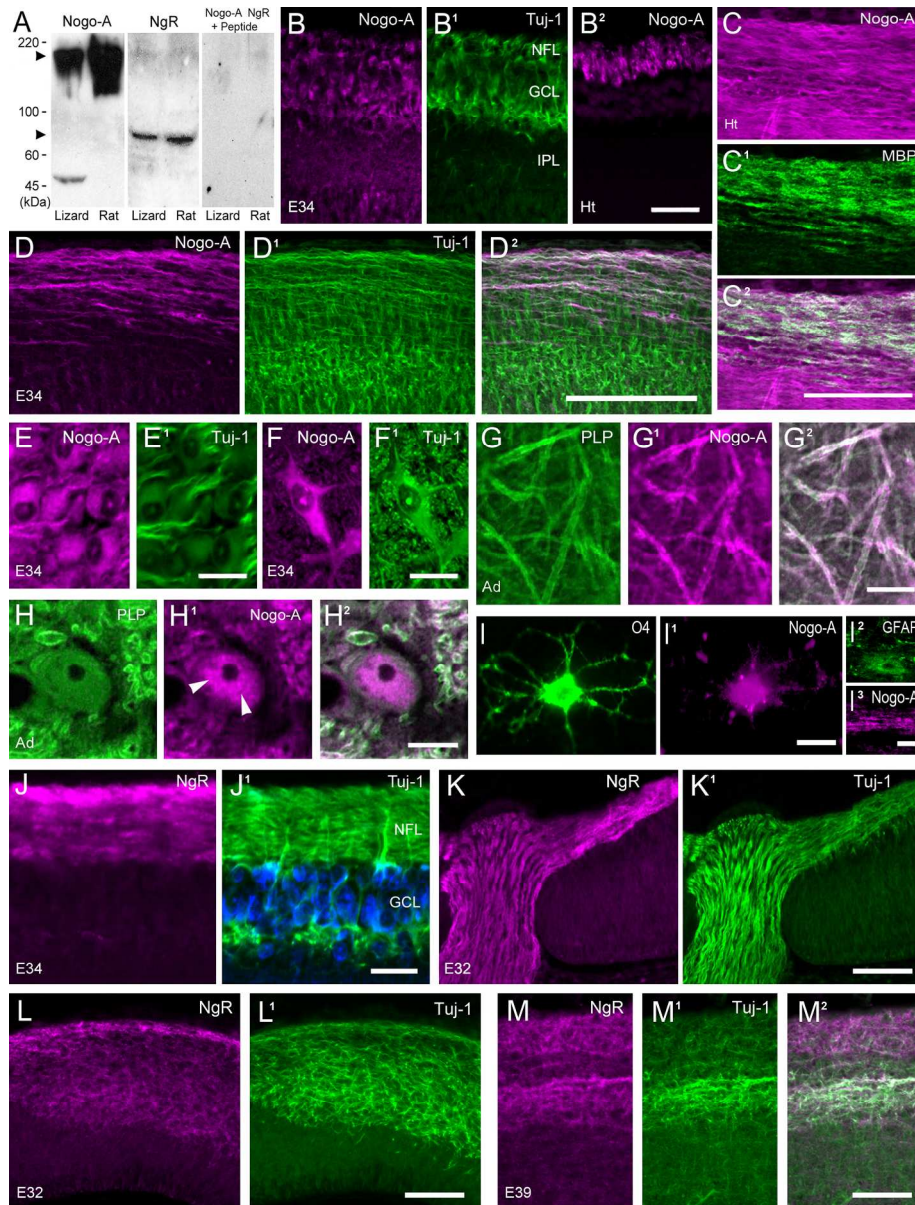


Figure 1: Expression of Nogo-A and NgR during ontogeny of the lizard nervous system. A: Western blot analysis in lizard and rat brain extracts using anti-Nogo-A and anti-NgR pABs. Each antibody recognizes a single protein band (arrowheads) at the appropriate apparent molecular weight (200 kDa for Nogo-A; 75 kDa for NgR) in lizard and rat brain. Detection of a putative degradation fragment of Nogo-A (around 50 kDa) in lizard samples is abolished by pre-adsorption of the antibody. B-B2: At E34, Nogo-A immunofluorescence is present in RGCs, the NFL and the IPL of the retina (B) as demonstrated by counterstaining with Tuj-1 (B1). At hatching stage, Nogo-A signal is restricted to the NFL (B''). C-C2: Nogo-A is detected in myelinated axons of the optic tract and adjacent unmyelinated axons in the hypothalamus (C). (C1) Myelination shown by MBP immunofluorescence, (C2) Signal overlay. (D, D1): Nogo-A is prominent in axons of the superficial retinorecipient layers of the optic tectum at stage E34 (D). (D1) Counterstain with Tuj-1, (D2) Signal overlay. E-F1: In stage E34 embryos, Nogo-A expression is prominent in the cytoplasm and processes of CNS (brain stem, F) and PNS (dorsal root ganglion, E) neurons, as confirmed by Tuj-1 labeling (F1, E1). The signal associated with nucleoli (arrowheads in E, F) is endogenous

fluorescence as also occurs in unstained sections. G-H2: In adult lizards, double-labeling with PLP (G) and Nogo-A (G') shows signal co-localization in myelinated axons (G2). PLP+ oligodendrocytes (H) display Nogo-A signal enriched in the cytoplasm, indicated by arrowheads in (H1), signal overlay shown in (H2). I-I3: O4+ lizard oligodendrocytes (I), but not GFAP+ astrocytes (I2) express Nogo-A (I1, I3). J-M'': During embryonic development, Tuj-1+ RGC axons (J1, K1, L1, M1) show distinct NgR labeling in the retinal NFL at stage E34 (J), in the ON (E32, K) and in the superficial and deep layers of the OT (E32 and E39, L and M, respectively). (M2) Signal overlay. Scale bars = 10 μ m in B-B2 and G-I3; 100 μ m in C-D2 and K-M2; 20 μ m in E-F1 and J-J1. GCL, ganglion cell layer; IPL, inner plexiform layer; NFL, nerve fiber layer.

210x276mm (300 x 300 DPI)

Accepted Article

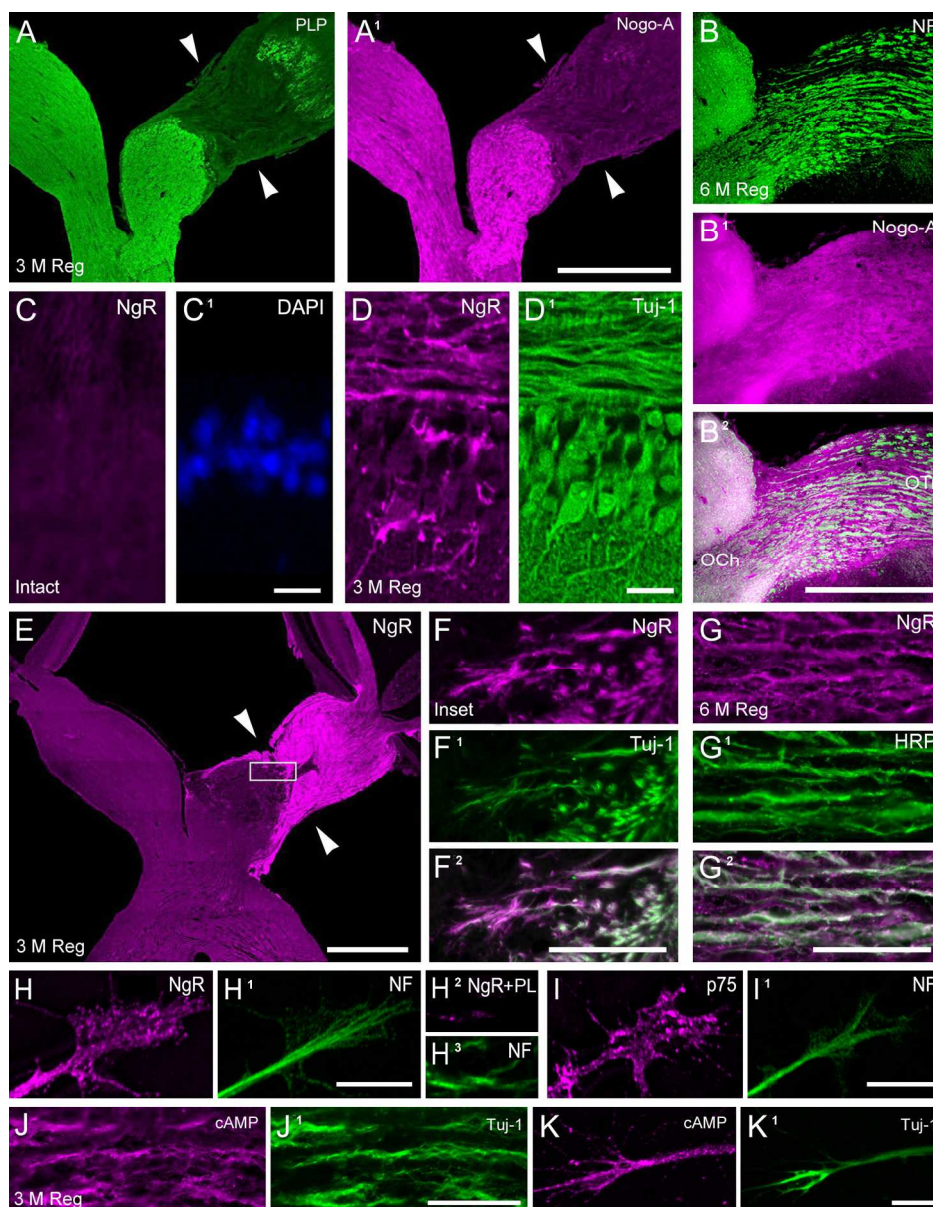


Figure 2: Changes of Nogo-A and NgR expression during regeneration of the lizard visual pathway. A-A1: PLP (A) and Nogo-A expression (A1) persist in the lizard visual pathway 3 months post injury, with the exception of the lesion site (marked by arrowheads). B-B2: At 6 months post injury, NF-positive bundles of regenerating axons (B) are traversing the Nogo-A-immunoreactive (B1) optic tract. (B2) Signal overlay. C-D1: NgR staining in RGCs is up-regulated (D) compared to the intact situation (C) after optic nerve injury, accompanied by elevated Tuj-1 immunoreactivity (D1). (C1) DAPI staining, indicating position of RGC nuclei. E: NgR is up-regulated in the regenerating optic nerve rostral to the lesion site 3 month post injury when RGC axons begin to traverse the injury site (indicated by arrowheads). F-F2: Details of the inset area in (E). NgR-positive regenerating axons (F) are identified by Tuj-1 labeling (F1). (F2) Signal overlay. G-G2: NgR up-regulation in regenerating RGC axons in the optic tract (G) is demonstrated by HRP tracing (G1) at 6 months post lesion. (G2) Signal overlay. H-I1: Lizard RGC growth cones regenerating *in vitro* express NgR (H) and its co-receptor p75 NTR (I). (H2) Phospholipase C treatment abolishes cell surface expression of NgR. (H1, H3, I1) Counterstaining and identification of neuronal structures with anti-NF Abs. J-J1: Elevated

cAMP staining (J) correlates with increased Tuj-1 immunofluorescence (J1) in regenerating lizard RGC axons distal to the lesion site at 3 months post lesion. K-K1: (K) cAMP immunoreactivity in lizard RGC growth cones extending on Nogo-A-Fc substrate in vitro, identified by Tuj-1 labeling (K1). (K2) Signal overlay. Scale bars = 500 μm in A-B2 and E; 10 μm in C-D1, H-I1 and K-K1; 20 μm in F-G2 and J-J1.

205x265mm (300 x 300 DPI)

Accepted Article

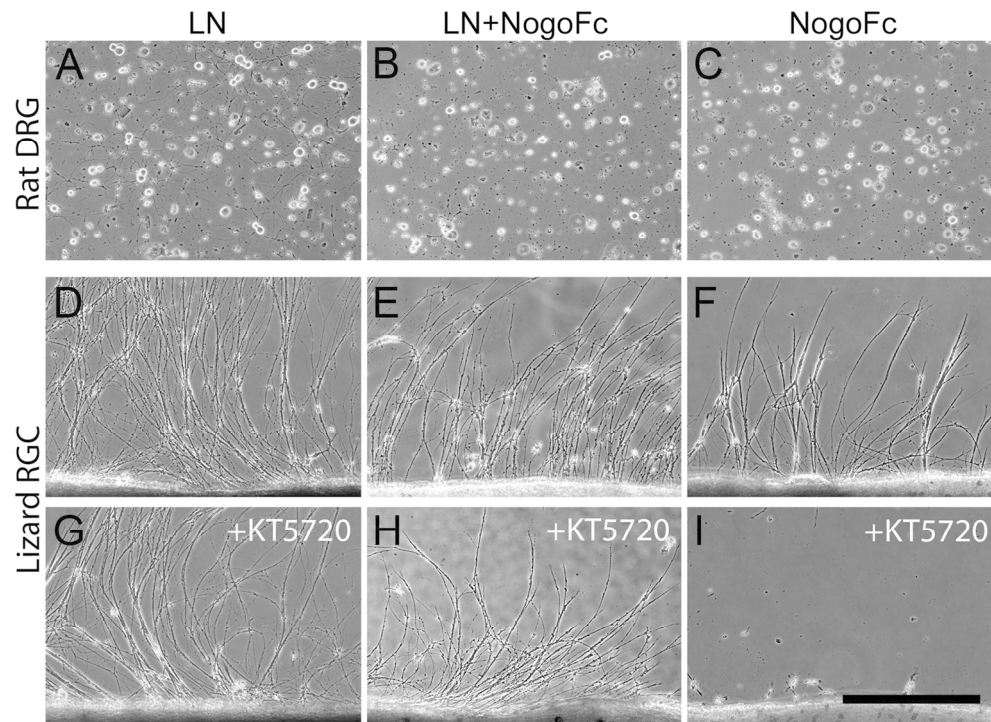


Figure 3: In vitro assays on neurite outgrowth in the presence of Nogo-A-Fc and the protein kinase A (pKA) inhibitor KT5720 (Typical results shown). Neonate rat DRG neurons (A-C) and lizard retinal explants (D-I) were cultured over 48 hr on substrates of polylysine/laminin (LN), polylysine/laminin with Nogo-A-Fc peptide (LN+NogoFc), or polylysine with Nogo-A-Fc (NogoFc). A-C: Rat DRG neurites grow profusely on LN (A), but presence of Nogo-A-Fc abolishes neurite growth on LN (B) and polylysine (C). D-F: Growth of lizard RGC axons is robust on LN (D), but also in presence of Nogo-A-Fc on LN (E) or on polylysine (F). G-I: Addition of KT5720 does not affect growth of lizard RGC axons on LN (G) or on LN with Nogo-A-Fc (H), but prevents axon growth on polylysine in the presence of Nogo-A-Fc (I). Scale bar = 100 μ m.

160x140mm (300 x 300 DPI)

Acc

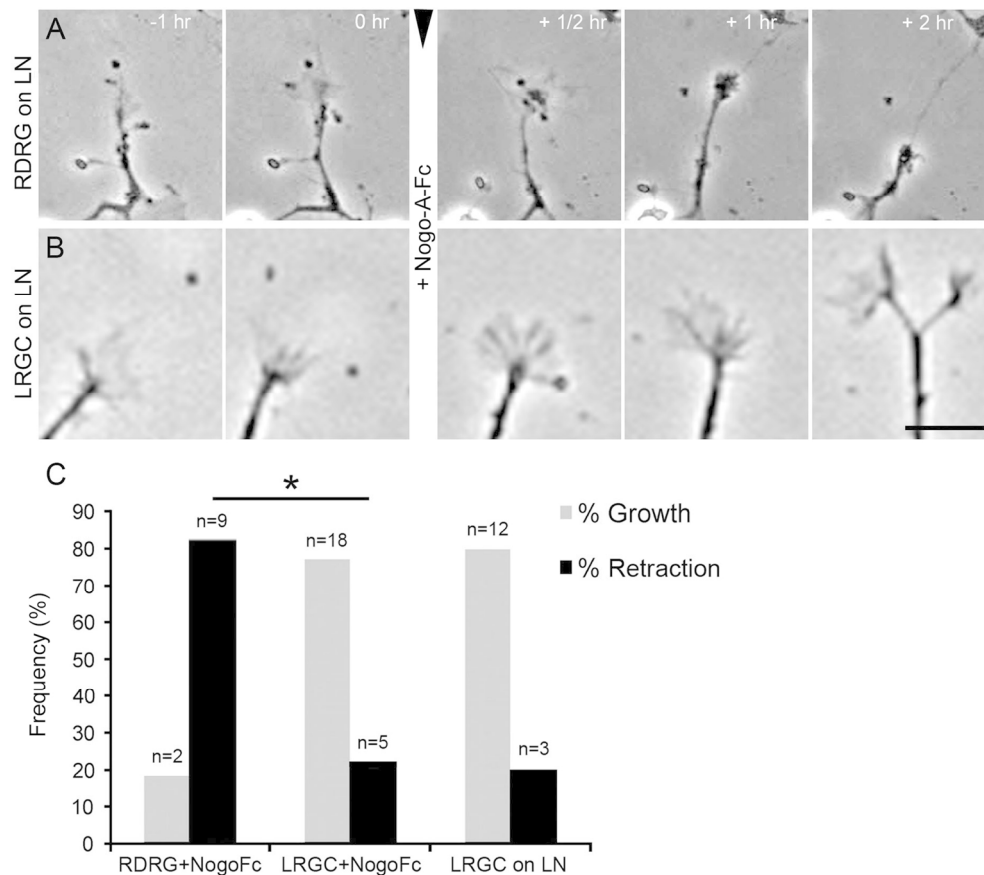


Figure 4: Collapse assay in neonate rat DRG (RDRG) and lizard retinal explants (LRGC) 3 months post-lesion. Explants were cultured on polylysine/laminin (LN), soluble Nogo-A-Fc added to the medium and time series of growth cone responses recorded. Phase contrast images were taken 1 hour before (-1 hr), at the time (0 hr) and 1/2hr, 1hr and 2 hr. after the addition of Nogo-A-Fc. Series (A): Typical collapse and retraction response of rat DRG growth cone after addition of Nogo-A-Fc. Series (B): Typical response of lizard RGC growth cones, which fail to collapse and retract after exposure to Nogo-A-Fc. C: Quantification of growth cone responses. Nogo-A-Fc causes collapse and retraction in rat DRG growth cones (RDRG + NogoFc), but fails to elicit collapse and retraction in lizard RGC axons (LRGC + NogoFc) beyond the spontaneous growth cone retraction rate of lizard RGC axons on polylysine/laminin (LRGC on LN). Asterisk denotes significant difference in the responses of RDRG vs LRGC growth cones in the presence of Nogo-A-Fc. (Chi-Square Test, $p \leq 0.05$). n, number of observed growth cones, derived from two (rat DRG neurons) and three (lizard RGC axons) independent experiments, respectively. Scale bar = 10 μ m

160x141mm (300 x 300 DPI)

AC

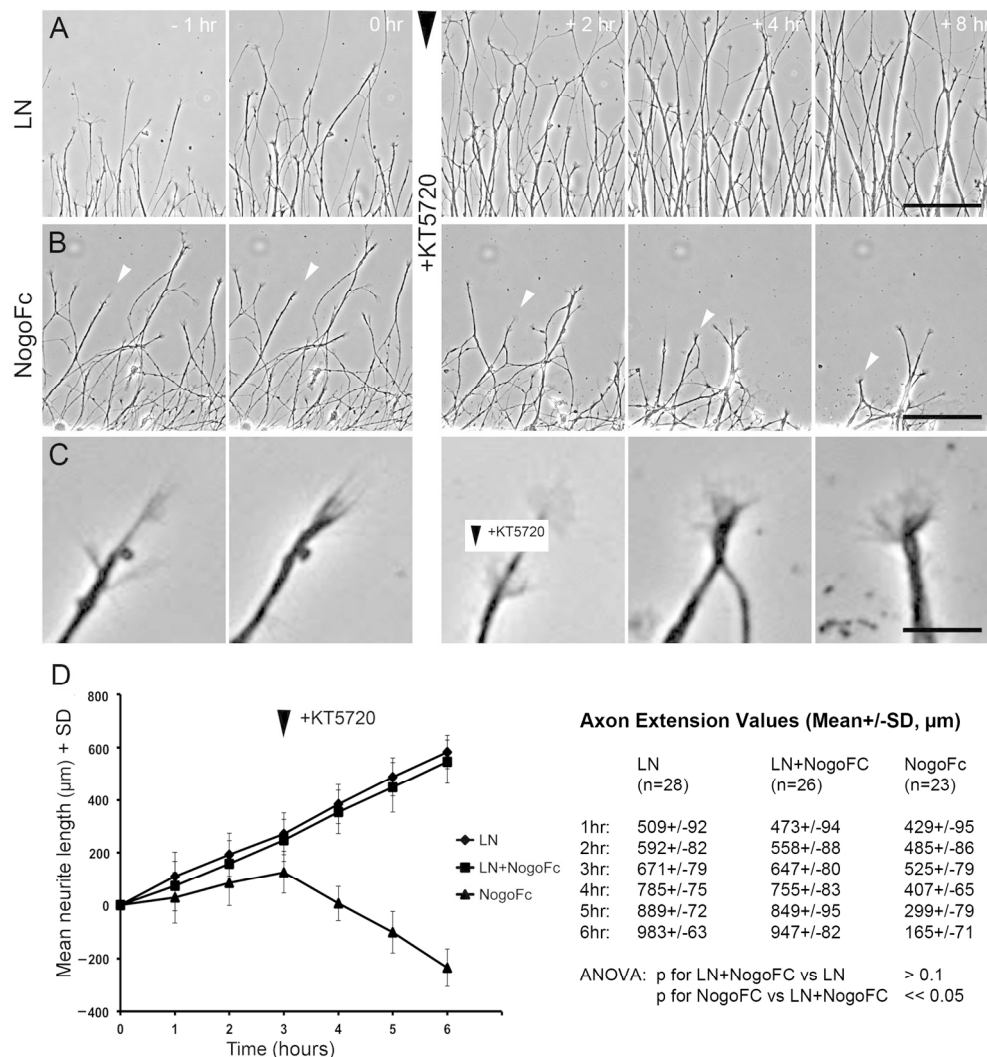


Figure 5: Time lapse analysis of the effect of the pKa inhibitor, KT5720 on lizard RGC axon growth in vitro. Retinal explants were placed on substrates of polylysine/laminin (LN, series A) or polylysine with Nogo-A-Fc (NogoFc, series B). KT5720 was added at the time point 0 (indicated by black arrowhead) and phase contrast time series were recorded between up to 3 hour before and up to 8 hr after addition of KT5720.

Series A: Axons on polylysine/laminin continue to grow after addition of KT5720. Axon growth on polylysine/laminin with Nogo-A-Fc (LN+NogoFc, not shown) is not significantly slower and equally unaffected by KT5720 (quantified in D). Series B: RGC axons on polylysine with Nogo-A-Fc, retract upon addition of KT5720 (see quantification in D). Series C: Higher magnification detail of growth cones indicated by arrowheads in B. KT5720, while causing axon retraction on Nogo-A-Fc, does not elicit collapse of spread growth cones to a significant extent and growth cone motility is maintained. D: Quantification of axonal length expressed as mean \pm standard deviation (SD). n, number of observed events. Scale bars = 100 μ m in A and B; 10 μ m in C.

172x184mm (300 x 300 DPI)

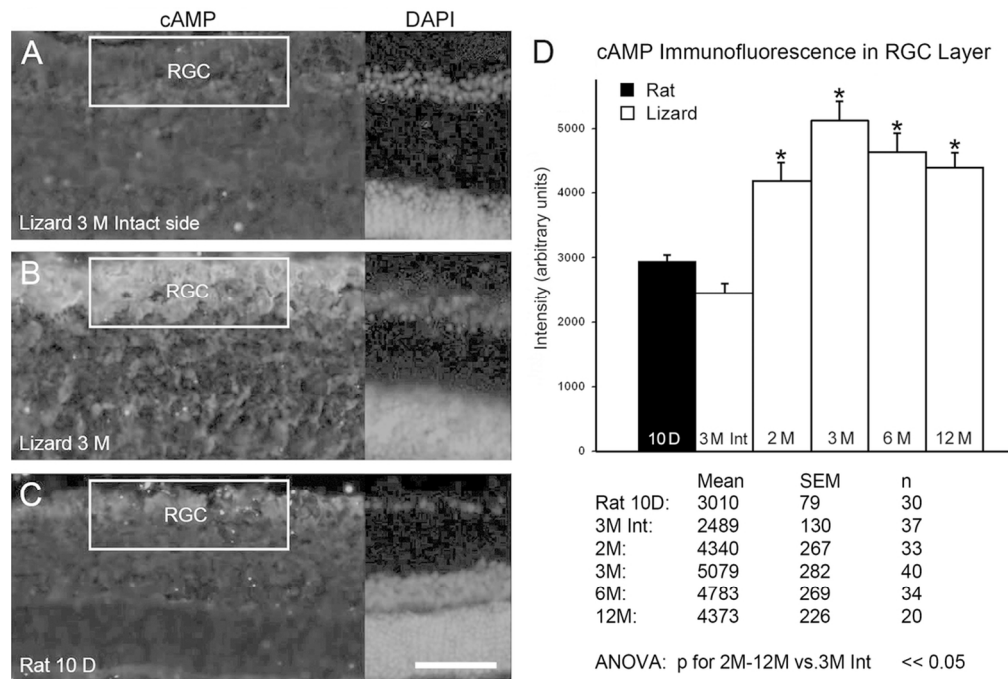


Figure 6: Immunohistochemical determination of cAMP levels in lizard and rat RGCs after optic nerve transection. Position of RGC nuclei is indicated by DAPI counterstaining. A-B: At 3 months postlesion, the contralateral (intact) lizard retina shows weak staining (A) whereas intensity of anti-cAMP immunofluorescence increases in the damaged RGCs (B). C: Rat RGCs did not show sustained increase of cAMP levels after 10 days postinjury. Boxes in A-C indicate size of areas used for intensity measurements in D. D: Quantification of cAMP immunofluorescence signal in the RGC layer. Densitometric measurements are represented as grayscale values on an arbitrary scale provided by the image analysis software. Intensities were significantly increased (One-Way ANOVA, $p < 0.05$) in the damaged lizard RGCs throughout the observed regeneration period between 2-12 months postlesion (asterisks), over control-like levels (contralateral/intact side) and over cAMP immunofluorescence levels observed in the rat RGCs 10 days postlesion. Data are representative of three different animals per group. Error bars indicate SEM. Scale bar = 50 μ m. D, days postlesion; Int, contralateral intact retina; M, months postlesion; n, number of measurements.

108x72mm (300 x 300 DPI)

Acc

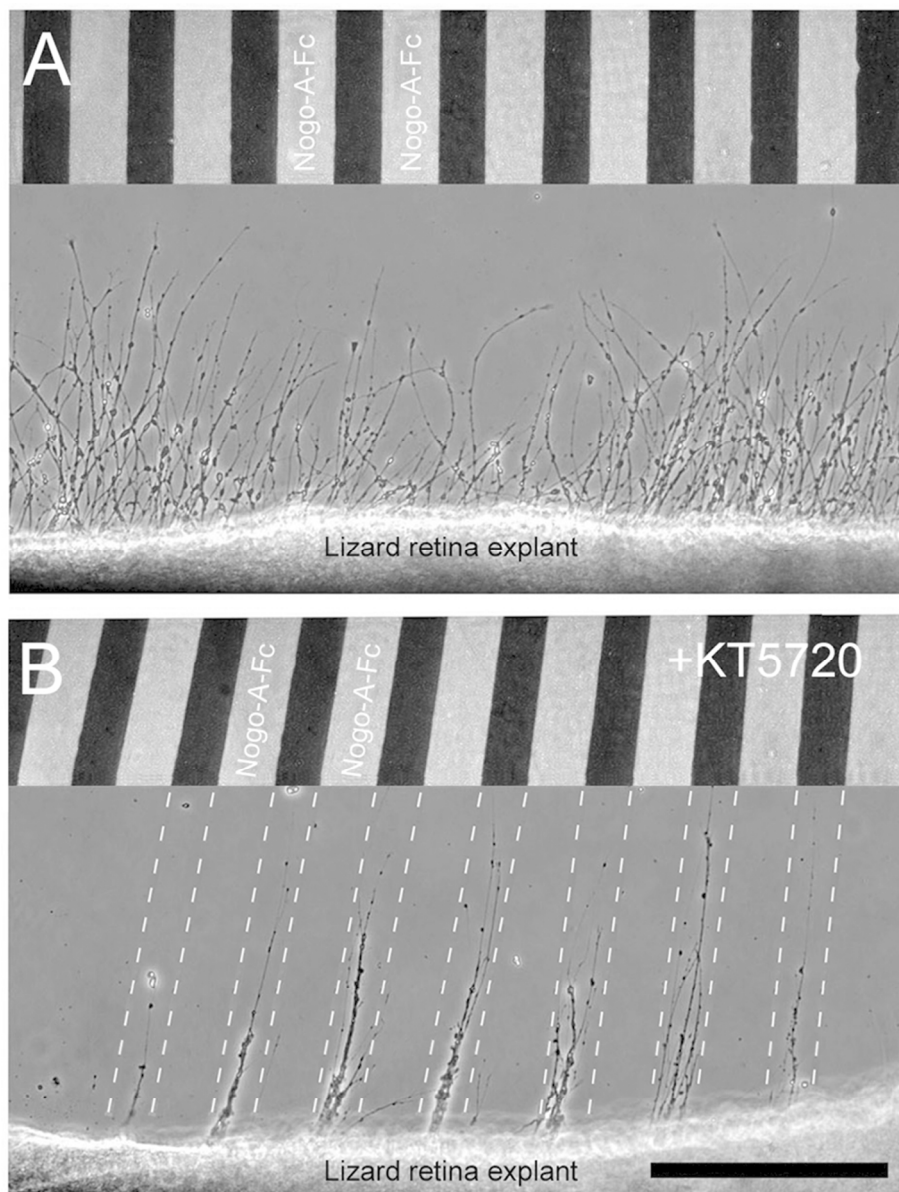
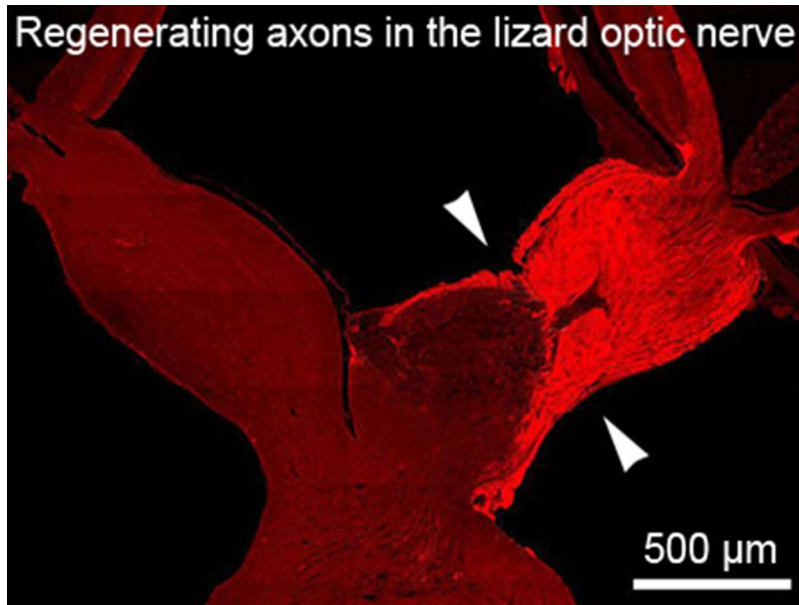


Figure 7: In vitro choice assay of growing axons from lizard retinal explants (Typical results shown). Nogo-A-Fc peptide was applied to polylysine-coated coverslips in a striped pattern and the coverslips overlaid with laminin. Axon outgrowth from lizard retinal explants on this patterned substrate was observed in the absence (A) and presence of the pKA inhibitor, KT5720 (B) in the medium. A: Lizard RGC axons do not distinguish between stripes with (grey) and without Nogo-A-Fc (black) in the absence of KT5720. B: In the presence of KT5720, axons become restricted to the stripes free of Nogo-A-Fc (black). Dashed lines delineate the adjacent stripes in the phase contrast image. Presence of Nogo-A-Fc is shown by immunostaining with anti-Nogo-A antibody (grey stripes). Scale bar = 100 μ m.

80x104mm (300 x 300 DPI)



141x105mm (72 x 72 DPI)

Accepted

Accepted Article

The authors show that the neurite growth inhibitory protein, Nogo-A and its receptor, NgR are expressed in a mammalian-like pattern in the lizard visual system, but Nogo-A does not inhibit lizard retinal axon regeneration. The findings indicate a crucial role for cAMP/pkA signaling in enabling axon regrowth in the lizard.